https://doi.org/10.5194/acp-2021-552
Preprint. Discussion started: 5 January 2022

Atmospheric Chemistry and Physics Discussions

Evaluation of WRF-CHIMERE coupled models for the simulation of $PM_{2.5}$ in large East African urban conurbations.

Andrea Mazzeo[1,2], Michael Burrow[1], Andrew Quinn[1], Eloise A. Marais[3], Ajit Singh[2], David Ng'ang'a[4], Michael J. Gatari[4], and Francis D. Pope[2]

1. School of Civil Engineering, University of Birmingham, Birmingham UK
2. School of Geography Earth and Environmental Sciences – GEES, University of Birmingham, Birmingham UK
3. Department of Geography, University College London, London, UK.
4. Institute of Nuclear Science and Technology, University of Nairobi, Nairobi, Kenya

Correspondence to Andrea Mazzeo (a.mazzeo@bham.ac.uk)

Abstract: *Urban conurbations of East Africa are affected by harmful levels of air pollution. The paucity of local air quality networks and the absence of capacity to forecast air quality make difficult to quantify the real level of air pollution in this area. The chemistry-transport model CHIMERE has been coupled with the meteorological model WRF and used to simulate hourly concentrations of Particulate Matter $PM_{2.5}$ for three East African urban conurbations: Addis Ababa in Ethiopia, Nairobi in Kenya, and Kampala in Uganda. Two existing emission inventories were combined to test the performance of CHIMERE as an air quality tool for a target monthly period of 2017 and the results compared against observed data from urban and rural sites. The results show that the model is able to reproduce hourly and daily temporal variability of aerosol concentrations close to observations both in urban and in rural environments. CHIMERE's performance as a tool for managing air quality was also assessed. The analysis demonstrated that despite the absence of high-resolution data and up-to-date biogenic and anthropogenic emissions, the model was able to reproduce 66-99% of the daily $PM_{2.5}$ exceedances above the WHO 24-hour mean $PM_{2.5}$ guideline (25 µg m^{-3}) in the three cities. An analysis of the 24-hour mean levels of $PM_{2.5}$ was also carried out for 17 constituencies in the vicinity of Nairobi. This showed that 47% of the constituencies in the area exhibited a low air quality index for $PM_{2.5}$ in the unhealthy category for human health exposing between 10000 to 30000 people/km^2 to harmful level of air contamination.*

Keywords: Air quality, East Africa, Particulate Matter, Anthropogenic emissions, numerical modelling, Air Quality Index

1 Introduction

The world's population has grown rapidly by 1 billion people in the last 12 years, reaching 7.9 billion in 2021. Future projections suggest a continuing annual increase of 1.8 %, meaning the global population will reach 8.5 billion by 2030, 9.7 by 2050, and 11.2 by 2100 (WPP, 2015). The African continent is predicted to have the fastest growing population rate in the world, and it is projected to double between 2010 and 2050, surpassing two billion (WPP, 2011). In addition to this a 60 % increase in population has been predicted by 2050, specifically in urban areas (WPP, 2012).

Population in Sub-Saharan East African (SSEA) countries have increased drastically since 1991 to 2019. In that period of time and according to data from the World Bank database (https://data.worldbank.org/), the Kenyan population grew from 24 to 52 million, the Ugandan population from 17 to 44 million and the Ethiopian population from 50 to 112 million. These increases in population were accompanied by a similar rate of increase in road transport, industrial activities and in the use of solid fuels (e.g. woods, charcoal and agricultural residues) for cooking purposes in urban areas (Bockarie et al., 2020;Marais et al., 2019).

As a result of these population increases, air quality of the urban areas of these countries, historically influenced by the large presence of seasonal burning biomass emissions (Haywood et al., 2008;Lacaux, 1995;Liousse et al., 2010;Thompson A. M., 2001), is progressively degrading (Marais and Wiedinmyer, 2016). This, in combination with the expanding urban population, has greatly increased the exposure of citizens to harmful Particulate Matter (PM) pollution with an aerodynamic diameter smaller than 10 and 2.5 µm (PM_{10} and $PM_{2.5}$, respectively) (Gatari et al., 2019;Kinney et al., 2011;Li et al., 2017;UN-Habitat, 2017).

Several diseases have been attributed to PM exposure in SSEA, including cardiovascular and cardiopulmonary diseases, cancers and respiratory deep infections (Dalal et al., 2011;Mbewu, 2006;Parkin et al., 2008). In 2012, the World Health Organization (WHO) estimated that in 2012 176,000 deaths in SSEA were directly connected to air pollution(WHO, 2012). Modelling studies have also found that exposure to outdoor air pollution has led to 626,000 disability-adjusted life per year (DALYs) in SSEA alone (Amegah and Agyei-Mensah, 2017), highlighting that these numbers could be much higher considering the limited amount of air quality data emanating from the region that are available for research purposes.

Considering the likely severe impacts of air pollution on human health in SSEA, the research interest in understanding air pollution trends in East Africa has increased in recent years. Many researchers have analysed the level of contaminations by short-term measurement campaigns (Amegah and Agyei-Mensah, 2017;deSouza P., 2017;Egondi et al., 2013;Gaita et al., 2014;Gatari et al., 2019;Kume, 2010;Ngo et al., 2015;Pope et al., 2018;Schwander et al., 2014;Vliet, 2007;Singh et al., 2021). Other studies observed annual average $PM_{2.5}$ concentrations in the order of 100 µg m^{-3} quantified in a small number of urban areas of SSEA (Brauer et al., 2012). These levels are about four times higher than the 24-hour average and ten times higher than the annual average WHO guidelines for $PM_{2.5}$ (Avis W. and Khaemba W., 2018;WHO, 2016) and underline that air pollution is a serious problem in this area of the world. A recent study by Singh et al. (2020), using visibility as a proxy for PM, showed that air quality in Addis Ababa, Kampala and Nairobi has degraded alarmingly over the last 4 decades.

The lack of lon-term air quality monitoring networks in many African countries have made it difficult to have reliable long-term air quality data (Petkova, 2013;Pope et al., 2018;Singh et al., 2020) and still little is known about the levels of air contamination in large urban conurbations (Peña, 2017). The paucity and sometimes complete absence of reliable data on air pollution levels makes it difficult to quantify the magnitude of the problem. Consequently, it is difficult for local and national authorities to plan possible improvement measures for the mitigation of anthropogenic emissions. Even if important steps forward have been made to improve the

https://doi.org/10.5194/acp-2021-552
Preprint. Discussion started: 5 January 2022

knowledge relative to anthropogenic emissions and emission inventories for Africa used for numerical simulations and forecasts of air quality (Assamoi and Liousse, 2010;Liousse, 2014;Marais and Wiedinmyer, 2016) the lack of surface observations to validate the emission magnitude and the simulated concentrations make these inventories susceptible of large error.

In this work we present the results of the implementation of a modelling system for meteorology and chemistry-transport processes to simulate the air quality levels of particulate matter $PM_{2.5}$ in the capital cities of Kenya, (Nairobi), Ethiopia (Addis Ababa) and Uganda (Kampala) and its validation against observation data. For Nairobi, we compare model outputs with observations from rural and roadside sites observations collected during the "A Systems approach to Air Pollution in East Africa" research project (ASAP-East Africa - www.asap-eastafrica.com, hereafter called ASAP) (Pope et al., 2018). For Addis Ababa and Kampala, the model was validated using hourly observations of $PM_{2.5}$ collected by the respective US Embassies.

Moreover, we assess the suitability of the chemistry-transport model as a decision support tool for policy makers to plan possible mitigation policies oriented to quantify the real level of air pollution in urban areas and quantify the human exposure to $PM_{2.5}$. Specifically, in terms of the accuracy of the model in estimating the daily WHO threshold limit exceedances of $PM_{2.5}$ in the three urban conurbations. For the particular case of Nairobi, we evaluate the average air quality indices by local constituency for the whole analysed period giving a new insight of the real level of air contamination in Nairobi to the general public and the relative population density exposed to harmful level of air contamination.

2 Material and Methods

To correctly describe the impact of anthropogenic emissions on urban air quality of Nairobi, Kampala and Addis Ababa, industrial and on-grid power generation emissions from the Emissions Database for Global Atmospheric Research (hereafter EDGAR) (Crippa M., 2018) inventory are combined with non-industrial, prominent combustion sources from the Diffusive and Inefficient Emission inventory for Africa (hereafter DICE) (Marais and Wiedinmyer, 2016). EDGAR, version 4.3.2, is a global inventory developed for year 2012 and DICE is a regional inventory for 2013. DICE includes important sources in Africa (i.e. motorcycles, kerosene use, open waste burning, and ad hoc oil refining, among others) that are absent or misrepresented in global inventories. Both inventories represent the most up-to-date anthropogenic emissions available for East Africa at the time of developing the local air quality model for this work.

EDGAR and DICE were combined to simulate the main chemical patterns between the 14^{th} of February and the 14^{th} of March 2017. The modelling system was validated for meteorological surface variables (temperature, relative humidity, wind speed and direction) and for hourly and daily concentration levels of $PM_{2.5}$. The period of simulation was chosen to align with the period of available data sampled from an airborne particulate matter monitoring campaign carried out in Nairobi as part of the ASAP project (Pope et al., 2018). Data from two different observation sites were chosen for the validation. These were the urban roadside sample site of Tom Mboya Street in Nairobi (1.28° S, 36.82° E) and the rural background site of Nanyuki (0.01°N, 37.07°E) (Pope et al., 2018). Hourly concentration of $PM_{2.5}$ used to compare the CHIMERE configuration applied to Kenya with Ethiopia and Kampala, were taken from two urban background sites corresponding to the US Embassies in Addis Ababa (9.05° N, 38.76° E) and Kampala (0.30° N, 32.59° E), respectively.

For the validation, all the available hourly observations for meteorology and chemistry were used. However, for the meteorological data only surface observations were available every three hours and the validation of the model in the vertical direction was not possible due to the lack of reliable vertical observed data for the simulated period.

2.1 Meteorological model WRF

The Weather Research and Forecasting (WRF) model is a numerical model for weather predictions and atmospheric simulations and is used commercially and for research purposes, including by the US National Oceanic and Atmospheric Administration (Powers, 2017;Skamarock, 2008).

Meteorology for driving CHIMERE was modelled using WRF by three geographical domains at different resolutions (from 18×18 km to 2×2 km) and a vertical domain divided into 30 levels, nine of which are below 1500 m. The first external domain has a spatial resolution of 18×18 km (Figure 1), with three nested domains at a resolution of 6×6 km centred on the three countries of interest (Figure 1, white squares). Three further nested domains with a resolution of 2×2 km were centred on Addis Ababa, Kampala, and Nairobi (Figure 1, white dashed squares and Figure 3a, b, c) and are the focus of the analysis.

The configuration adopted for the WRF simulations has been chosen according to previous works made on East Africa (Kerandi et al., 2016;Kerandi et al., 2017;Pohl et al., 2011) and is summarized in Table 1. The Yonsei University Scheme (YSU - (Hong S., 2006)) was chosen to represent the Planetary Boundary Layer while the Community Atmosphere Model (CAM - (Collins, 2004)) was used for the long and short-wave radiation scheme. Initial and boundary conditions for the external coarse domain at 18×18 km were obtained from the NCEP FNL (Final) Operational Global Analysis data (Wu, 2002). Boundary condition for the first (6×6 km) and second (2×2 km) nest domains were taken from the respective parent domains using the two-way-nesting approach. The process enables the lateral conditions for the internal domains to be calculated from the outputs of the respective parent domains at lower resolution at every time step of the simulation.

The Land use option chosen for the simulations was based on NOAH (Tewari, 2004) while the WRF Single–moment 3–class Scheme (WSM3) for clouds and ice proposed by Hong S. (2004) was chosen for the reproduction of the microphysical processes in WRF.

https://doi.org/10.5194/acp-2021-552
Preprint. Discussion started: 5 January 2022

Atmospheric Chemistry and Physics Discussions

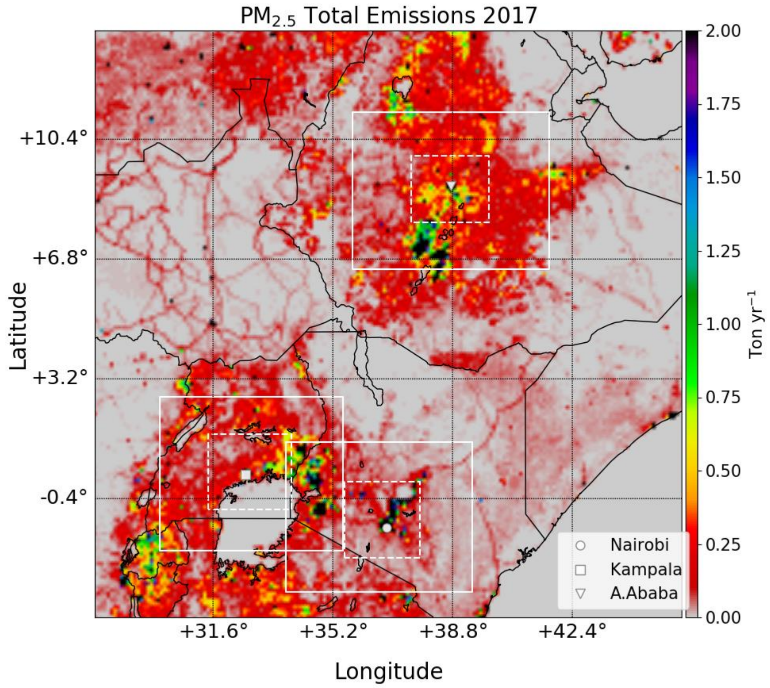

Figure 1: *Spatial distribution of the $PM_{2.5}$ emissions from DICE-EDGAR merged emission inventory for East Africa for the WRF domain at 18×18 km of resolution. The continuous white lines show the location of the first nested domain at 6×6km of resolution used in WRF-CHIMERE. The dashed white squares give the locations of the second nested domains at 2×2km centred on Addis Ababa (Ethiopia), Kampala (Uganda) and Nairobi (Kenya) used for WRF-CHIMERE.*

2.2 The CHIMERE Chemistry Transport model

CHIMERE, version 2017r4 (Mailler et al., 2017), is a Eulerian numerical model for reproducing three-dimensional gas-phase chemistry and aerosols processes of formation, dispersion and deposition over a defined domain with flexible spatial resolutions. CHIMERE has been used for a number of comparative research studies of Ozone and particulate matter PM_{10} from the continental scale, (Bessagnet et al., 2016;Zyryanov et al., 2012) to the urban scale (van Loon et al., 2007;Vautard et al., 2007). Furthermore, the model has been used for event analysis, scenario studies (Markakis et al., 2015), forecasts, and impact studies of the effects of air pollution on health (Valari and Menut, 2010) and vegetation (Anav et al., 2011). The authors highlight that the version of CHIMERE adopted is the 2017r4, the most recent available at the time when the present work was realized.

The configuration adopted in this work uses initial and boundary conditions from the global three-dimensional chemistry-transport model (LMDz-INCA, (Hauglustaine et al., 2004)), both for gaseous pollutants and for aerosols for the most external domain at 6 km of resolution while for the most internal domains at 2 km of resolution, the boundary conditions are calculated from model outputs of the parent domains. The complete chemical mechanism used for all the simulations was SAPRC-07-A (Carter, 2010) which can describe more than

https://doi.org/10.5194/acp-2021-552
Preprint. Discussion started: 5 January 2022

Atmospheric Chemistry and Physics Discussions

275 reactions of 85 species. SAPRC-07-A is the most recent chemical mechanism available for CHIMERE version 2017r4.

Horizontal and vertical diffusion is calculated using the approach suggested by Van Leer (1979) and the thermodynamic equilibrium ISORROPIA model (Nenes, 1998) is used for the particle/gases partitioning of semi-volatile inorganic gases. The model permits calculation of the thermodynamical equilibrium between sulphates, nitrates, ammonium, sodium, chloride and water dependent upon temperature and relative humidity data.

Radiative transfer processes are accounted in CHIMERE using the Fast-JX model (Wild, 2000;Bian, 2002). Fast-JX is applied also in other models (Voulgarakis, 2009;Real and Sartelet, 2011;Telford et al., 2013). The photolysis rates calculated by Fast-JX model are validated both inside the limits of the boundary layer (Barnard, 2004) and in the free troposphere (Voulgarakis, 2009).

Secondary organic aerosols (SOAs), including biogenic and anthropogenic precursors, have been modelled in CHIMERE as described by (Pun, 2006). SOAs formation is represented as a single-step oxidation of the precursors, differentiating hydrophilic by hydrophobic SOAs in the partitioning formulation. Finally, biogenic emissions were taken in account within CHIMERE using MEGAN model outputs as described by (Guenther, 2006).

Table 1: *Main configuration parameters adopted for the modelling system WRF-CHIMERE for all simulations.*

WRFv3.9.1 Configuration		
Initial and Boundary conditions	GFS FNL- Reanalysis	*Wu (2002)*
PBL Parametrization	YSU	*Hong S. (2006)*
SW/LW Radiation Scheme	CAM	*Collins (2004)*
Land Use	NOAH	*Tewari (2004)*
Micro Physics Scheme	WSM3	*Hong S. (2006)*
Vertical Levels	30	
CHIMERE2017 Configuration		
Initial and boundary conditions	LMDz-INCA	*Hauglustaine et al. (2004)*
Anthropogenic Emissions	EDGARv3.4.1 + DICE-Africa	*Crippa M. (2018);Marais and Wiedinmyer (2016)*
Biogenic Emissions	MEGAN	*Guenther (2006)*
Gas/Aerosol Partitions	ISORROPIA	*Nenes (1998)*
Secondary Organic Aerosols	1	*Pun (2006)*
Radiative Transfer	Fast-JX	*Wild (2000);Bian (2002)*
Chemistry Mechanism	SAPRC-07-A	*Carter (2010)*
Horiz. / Vert. Transport scheme	VanLeer	*Van Leer (1979)*
Vertical Levels	30	

2.3 Emission Inventories

The emission inventories used for the simulation of the anthropogenic emissions for East Africa were the EDGARv4.3.2 global inventory for the year 2012 (EDGAR) and the Diffuse and Inefficient Combustion Emissions in Africa inventory for the year 2013 (DICE). Both inventories were the most up to date available at the time of the analysis, have the same spatial resolution of 0.1×0.1 ° and provide the annual total of anthropogenic emissions for relevant gases and aerosols.

EDGAR provides emissions data for CO, NO, NO_2, SO_2, NH_3, NMVOCs, BC, OC, PM_{10} and $PM_{2.5}$ as an annual total divided by the sector according to the IPCC-1996 classification. All human activities with exception of large-scale biomass burning are included in EDGAR (Crippa M., 2018).

DICE provides emissions from particular diffuse and inefficient combustion emission sources (road transport, residential biofuel use, energy production and charcoal production and use) for gaseous pollutants (CO, NO, NO_2, SO_2, NH_3, NMVOCs) and aerosols (BC, OC). Seasonal biomass burning that is considered a large pollution source in Africa is included in DICE as comparable emissions of black carbon and higher emissions of nonmethane volatile organic compounds. Emissions from DICE were used to provide annual total emissions for particular emission sources considered to be misrepresented or missing in a global inventory such as EDGAR.

The preparation of the final emission inventory was carried out in two steps. First, DICE and EDGAR inventories were merged, by pollutant and by sector, following the approach suggested by Marais and Wiedinmyer (2016). $PM_{2.5}$ emissions are included in DICE as individual components of organic carbon (OC) and black carbon (BC) but they need to be expressed as lumped $PM_{2.5}$ in CHIMERE. Therefore $PM_{2.5}$ was calculated as the sum of Organic Carbon (OC - originally present in DICE) multiplied for a conversion factor following Pai et al. (2020) to represent Organic Aerosols emissions and summed with Black Carbon (BC – originally present in DICE) as follows:

$$PM_{2.5} = (OC \times c) + BC \quad \text{Eq. (1)}$$

Secondly, the emisurf2016 pre-processor of CHIMERE was used to scale the emissions from the original resolution of 0.1×0.1 ° (~10 km) to the final resolution of each domain simulated (6×6 and 2×2 km) using population density data provided from the Socioeconomic Data and Application Centre (SEDAC) (http://sedac.ciesin.columbia.edu/) as proxy for the spatial distribution. SEDAC provides population density maps at high resolution (1×1 km) for the years 2010, 2015 and 2020. The SEDAC population density data calculated for most internal domains at 2×2 km (Figure 3a, b, c) suggest for 2010 a total population of 7 million for Nairobi, 4.8 million for Kampala and 4.5 million for Addis-Ababa. These totals grow respectively to 8.1, 5.9 and 5.0 million for 2015 and to 9.4, 7.3 and 5.7 million for 2020. The original SEDAC data were used for a linear extrapolation of the population density data to the target year 2017 and were used by emisurf2016 for the spatial allocation of the emissions. The resulting merged inventory (hereafter, DICE-EDGAR) totals by pollutant and sectors for the most external domain at 18x18km of resolution are shown in Figure 2.

https://doi.org/10.5194/acp-2021-552
Preprint. Discussion started: 5 January 2022

Atmospheric Chemistry and Physics Discussions

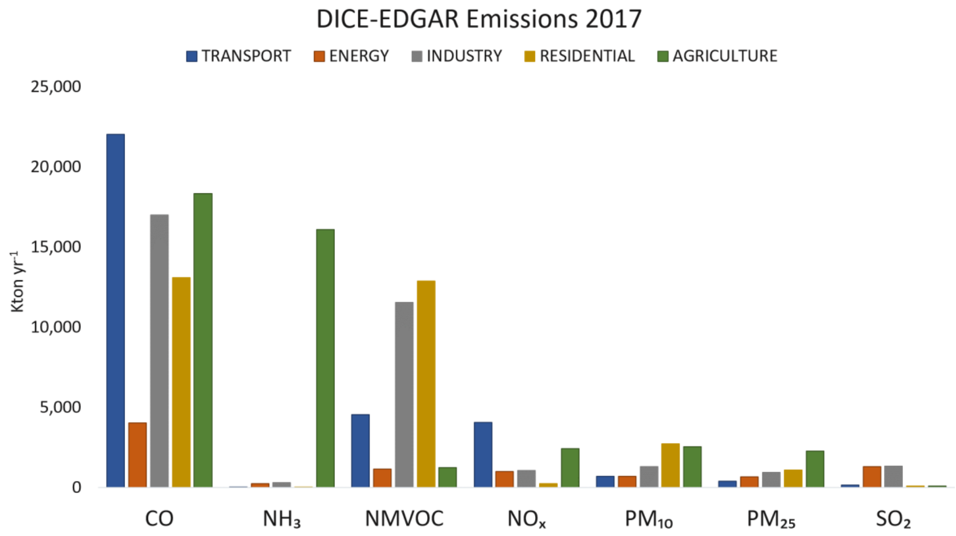

Figure 2: *Annual Totals for the merged emission inventory DICE-EDGAR for year 2017 calculated on the spatial domain at 18x18 km shown in Figure 1.*

Biogenic emissions and mineral dust considered in this work have been calculated in-line by CHIMERE. The former is calculated by MEGAN model outputs as described by Guenther (2006) while the latter are calculated using the USGS land use database provided by CHIMERE. The soil is represented by relative percentages of sand, silt, and clay for each model cell. The USGS database, called STATSGO-FAO accounts of 19 different soil types recorded in the global database with native resolution of 0.0083×0.0083 °. To have homogeneous datasets, the STATSGO-FAO data are re-gridded into the CHIMERE simulation grids. For mineral dust emission calculations, the land use is typically used to provide a desert mask specifying what surface is potentially erodible.

The emissions used in this work could still potentially not account for additional misrepresented or unaccounted sources due to the time difference between the age of the data in the EDGAR and DICE inventories and the observations used for the validation of the modelling system. The lack of up to date national emission inventories collected at a sufficient resolution, in addition to the lack of research sources providing projections of emissions for 2017, meant that it was not possible to generate more detailed information about the anthropogenic sources of emissions for East Africa.

It is noted that the time stamp of the anthropogenic emissions and the validation period are different. The emissions are relative to year 2013 while the observation used for the validation for 2017. In the absence of additional data and in the lack of national or local mitigation policies in the three countries we assume that the differences in time stamp do not make large difference to the emission estimates. More detailed analysis of the emission sources and the implementation of possible mitigation policies at national and local levels could in future change this situation.

https://doi.org/10.5194/acp-2021-552
Preprint. Discussion started: 5 January 2022

Atmospheric Chemistry and Physics Discussions

2.4 Weather and Chemistry Observations

Observations for temperature, wind speeds and directions used for the validation of the WRF model were taken from the UK Met Office MIDAS database (https://www.metoffice.gov.uk/). Data from 11 weather stations, three for Ethiopia (hereafter ETH2K, Figure 3a) and Uganda (hereafter UGA2K, Figure 3b) and five for Kenya (hereafter KEN2K, Figure, 3c) were used to validate the simulations at a resolution of 2×2 km (Table 2).

The ground stations are at different altitudes above sea level to a maximum of 2355 m (i.e. the Harar Meda station in Ethiopia, n.2 in Figure 3, a). The validation was performed by comparing model outputs with observations for the variables, namely surface temperature, wind speed and direction and relative humidity. The latter, not originally available in the MIDAS dataset, was calculated using the coefficients proposed by Alduchov O. (1996) based on hourly surface and dew point temperatures observed values and then compared with modelled data obtained by WRF.

Hourly concentrations of $PM_{2.5}$ were used for the validation of CHIMERE for the three internal domains at 2×2 km (Figure 3a, b, c). For the urban area of Nairobi, data were provided by the calibrated sampling campaign performed by Pope et al. (2018) for the roadside site at Tom Mboya Street in Nairobi (1.28° S, 36.82° E). For the urban areas of Addis Ababa and Kampala, hourly concentration of $PM_{2.5}$ were obtained from the air quality monitoring stations of the two US Embassies in Ethiopia (9.05° N, 38.76° E) and Uganda (0.30° N, 32.59° E) using optical counters. Data from Uganda and Ethiopia were used to compare the configuration applied to CHIMERE for Kenya with the two other countries. Hourly concentrations from the rural site of Nanyuki, Kenya (0.01°N, 37.07°E) provided by the calibrated sampling campaign performed by Pope et al., (2018) were used to complement the validation of CHIMERE outside the urban area of Nairobi (Table 2).

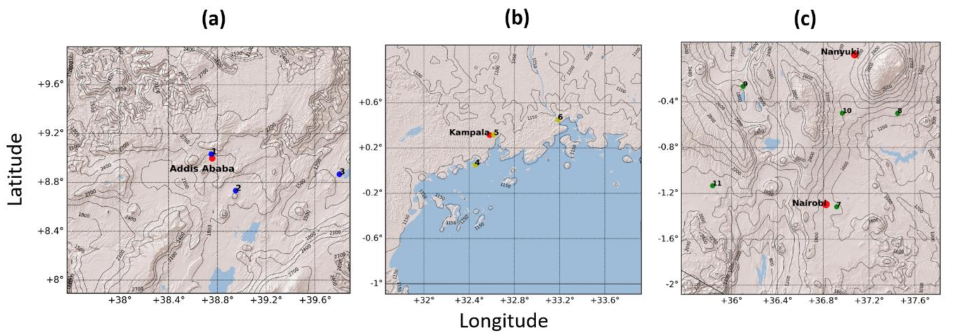

Figure 3: *Second-nested domains at a spatial resolution of 2×2 km centred on the cities of Addis Ababa (ETH2K - a), Kampala (UGA2K – b), Nanyuki and Nairobi (KEN2K - c) created using the WRF model. The red dots represent locations of $PM_{2.5}$ measurements. The blue, yellow and green dots refer to the location of the ground weather stations used for the meteorological validation in Ethiopia, Uganda, and Kenya, respectively. The numbers relate to the stations detailed in Table 2.*

https://doi.org/10.5194/acp-2021-552
Preprint. Discussion started: 5 January 2022

Table 2: MIDAS *ground weather stations used for the validation of the 2×2km domains. Station no. corresponds to the position of each station in Figure 3a, b and c and* $PM_{2.5}$ *observation points for the urban domains of Addis Ababa, Kampala and Nairobi used for the validation of CHIMERE model.*

Station n.	Domain	Name	Lat (°)	Lon (°)	Elev. (m a. g. l)
1	ETH2K	Addis – Bole	0.03	38.75	1900
2		Harar Meda	8.73	38.95	2355
3		Metehara	8.87	39.90	930
		US Embassy ($PM_{2.5}$ – urban background)	9.05	38.76	1900
4	UGA2K	Entebbe (Airport)	0.05	32.45	1155
5		Kampala	0.32	32.62	1144
6		Jinja	0.45	33.18	1175
		US Embassy ($PM_{2.5}$ – urban background)	0.30	32.59	1150
7	KEN2K	Nairobi (Airport)	-1.32	36.92	1624
8		Embu	-0.50	37.45	1493
9		Nakuru	-0.27	36.10	1901
10		Nyeri	-0.50	36.97	1759
11		Narok	-1.13	35.83	2104
		Tom Mboya Street ($PM_{2.5}$ – roadside)	-1.28	36.82	1795
		Nanyuki ($PM_{2.5}$ – rural background)	0.01	37.07	1947

3 Results and Discussion

The coupled WRF-CHIMERE model was run at spatial resolutions of 18×18, 6×6 and 2×2 km for meteorology and at 6×6 and 2×2 km for chemistry for the three domains of East Africa. The statistical analysis shown in the following sections describes the validation results for the three internal domains at a resolution of 2×2 km as these are the focus of the present work.

Ground weather stations from the MIDAS database, included in the 2×2 km domains of all countries, were analysed as individually, and shown as average of all stations. The time series and wind roses are relative to the closest stations from MIDAS database to each urban city centre of the three capital cities, namely Addis- Bole (n 1 in Table 2), Kampala (n 5 in Table 2) and Nairobi Airport (n 7 in Table 2).

Initially, the validation of CHIMERE focused on Kenya for which hourly concentrations of $PM_{2.5}$ were taken from two different sites (roadside and rural) from the field sampling campaign described by Pope et al., (2018). Secondly, the same configuration adopted for Kenya was used for Ethiopia and Uganda to test both the homogeneity of the emission rates on other urban conditions, and the configuration chosen for CHIMERE in different urban and environmental conditions. At this stage of the validation, a threshold limit of 25 µg m^{-3} for $PM_{2.5}$ per day provided by WHO (WHO, 2005) was used to quantify the number of exceedances observed and modelled by CHIMERE for the three cities.

The validation process was hindered by the highly variable quantity and quality of available meteorological data. The majority of the weather observations are provided on a 3-hourly basis, with varying amounts of missing data. Despite this the statistical evaluation for WRF has been performed comparing model and observations only when the latter were available. We recall that the objective of this work aims to test the performances of a modelling system for the simulation of air quality concentrations for East Africa, updating and using the available input data available and assessing the possible adoption of these tools for air quality policy making at this extent of the data.

3.1 Validation of the WRF simulations

In order to assess the performance of WRF in simulating surface temperature, relative humidity wind speed and direction, the model simulation outputs were compared with all the available ground weather station data available for the period of analysis, 14th of February to 14th of March 2017.

3.1.1 Statistical evaluation of WRF performances

A statistical analysis, in terms of the Mean Normalized Bias (MNB), Normalized Root Mean Square Error (NRMSE) and Pearson's coefficient (R), was carried out to compare modelled and observed values for the domain at 2×2 km resolution averaging the observed and modelled values on all the stations present on each domain (Table 3).

The results of the statistical analysis show that WRF is capable of reproducing the mean levels of surface temperature with a mean underestimation over the three domains of 1.4 and 1.5 °C for Ethiopia and Uganda and of 4.1 °C for Kenya. Relative humidity is overestimated by WRF in KEN2K of 0.2 % and underestimated in ETH2K of 6.4 % and in UGA2K of 7.5 % (Table 3). Wind Speed and directions for the three domains show respectively, the presence of northern winds in UGA2K correctly captured by the model with a difference of around 4 ° in comparison with the observations, an average eastern wind component in KEN2K partially reproduced by the model that allocate the average wind directions on a more south-eastern component of wind with a difference of around 40.2 ° while in ETH2K the average wind direction modelled and observed are close with a difference of 4.2 ° on a south-eastern component of prevailing wind. The observed and modelled wind speed in UGA2K and ETH2K are in reasonable agreement with a difference of 0.9 and 0.2 m s^{-1}, respectively, while the difference is higher for KEN2K, 7.4 m s^{-1} where the wind speed tends to be underestimated by the model (Table 3).

The MNB values (Table 3) for relative humidity and surface temperature are between -0.1 and 0.004, and -0.07 and -0.1, respectively showing the capability of WRF of reproducing the hourly variation of these two variables close to the observations. The MNB values for Wind speed and directions are respectively between 0.4 and 0.7 and between -0.03 and 13.7 showing the capability of WRF of reproducing the two components of wind despite the different topographic conditions in the three domains.

Similarly, the NRMSE suggests that the modelled and observed relative humidity and surface temperature are in good agreement. Ranging, for the former between 0.3 (UGA2K) and 0.5 (KEN2K) and founded for the latter as 0.2 for the three domains. The wind direction NRMSE is higher in KEN2K (8.1) and similar in the two other domains, between 1.0 and 1.4 while wind speed NRMSE is similar in the three domains, ranging between 0.9 in KEN2K and 1.3 in ETH2K.

https://doi.org/10.5194/acp-2021-552
Preprint. Discussion started: 5 January 2022

The calculated Pearson's coefficient (R) shows varying agreement between the model and observations of between 0.1 and 0.7 for the three domains. The highest R value for relative humidity of approximately 0.7 was obtained for ETH2K while the lowest R values occurred in UGA2K (0.3). Highest values of R for surface temperature were found in ETH2K (0.6), followed by KEN2K (0.5) and UGA2K (0.3). For wind speed, the highest R coefficient values are for the KEN2K (0.5) and the lowest for UGA2K (0.1) while for wind directions, the highest R value found was for UGA2K (0.3) with values of approximately 0.2 for the other two domains (Table 3).

Table 3: *Statistical analysis of relative humidity, surface temperature, wind speed and directions averaged on all the available weather stations for the second nested domains UGA2K, KEN2K and ETH2K at 2×2km of resolution. Mean observed and modelled values (ObsMean, ModelMean), mean normalized bias (MNB) normalized root mean square error (NMRSE) and Pearson's Coefficient (R) have been calculated.*

	Rel. Humidity			**Temperature**		
	UGA2K	**KEN2K**	**ETH2K**	**UGA2K**	**KEN2K**	**ETH2K**
ObsMean	68.2	63.1	51.3	24.5	23.2	22.7
ModelMean	60.7	63.3	44.9	23.0	19.1	21.3
MNB	-0.1	0.004	-0.1	-0.07	-0.1	-0.06
NRMSE	0.3	0.5	0.4	0.2	0.2	0.2
R	0.3	0.4	0.7	0.3	0.5	0.6
	Wind Dir			**Wind Speed**		
	UGA2K	**KEN2K**	**ETH2K**	**UGA2K**	**KEN2K**	**ETH2K**
ObsMean	6.8	91.5	104.0	2.5	11.2	3.5
ModelMean	2.8	131.7	99.8	3.4	3.8	3.7
MNB	-0.03	13.7	0.02	0.7	0.4	0.5
NRMSE	1.4	8.1	1.0	1.1	0.9	1.3
R	0.3	0.2	0.2	0.1	0.5	0.4

3.1.2 Hourly variation of Temperature and Relative humidity

The three MIDAS stations providing weather observations closest to the urban areas of the Addis Ababa, Kampala and Nairobi have been analysed individually in form of hourly time series of surface temperature and relative humidity and wind roses for wind speed and directions.

The hourly surface temperature and relative humidity are shown in Figure 4 for the three ground weather stations closest to the centre of the three cities: Addis-Bole (n.1 in Figure 3a), Kampala Station (n.5 in Figure 3b) and Nairobi (n.7 in Figure 3c).

The temperature range observed at the three stations was between 9 and 27° C for the Addis Bole Station, 16 and 31° C for Kampala and 16 and 33° C for Nairobi. By inspection of Figure 4, it can be seen that the WRF model is able to reproduce the main diurnal cycle of variation of temperature and relative humidity for the three ground weather stations. Surface temperature peaks are slightly underestimated by the model for the three stations with a small mean bias at the three stations between -0.06 and -0.1. The highest agreement between the model and

https://doi.org/10.5194/acp-2021-552
Preprint. Discussion started: 5 January 2022

Atmospheric Chemistry and Physics Discussions
Open Access
EGU

observation is for Kampala while the model tends to underestimate the diurnal peaks of surface temperature almost systematically for Addis-Bole and Nairobi stations.

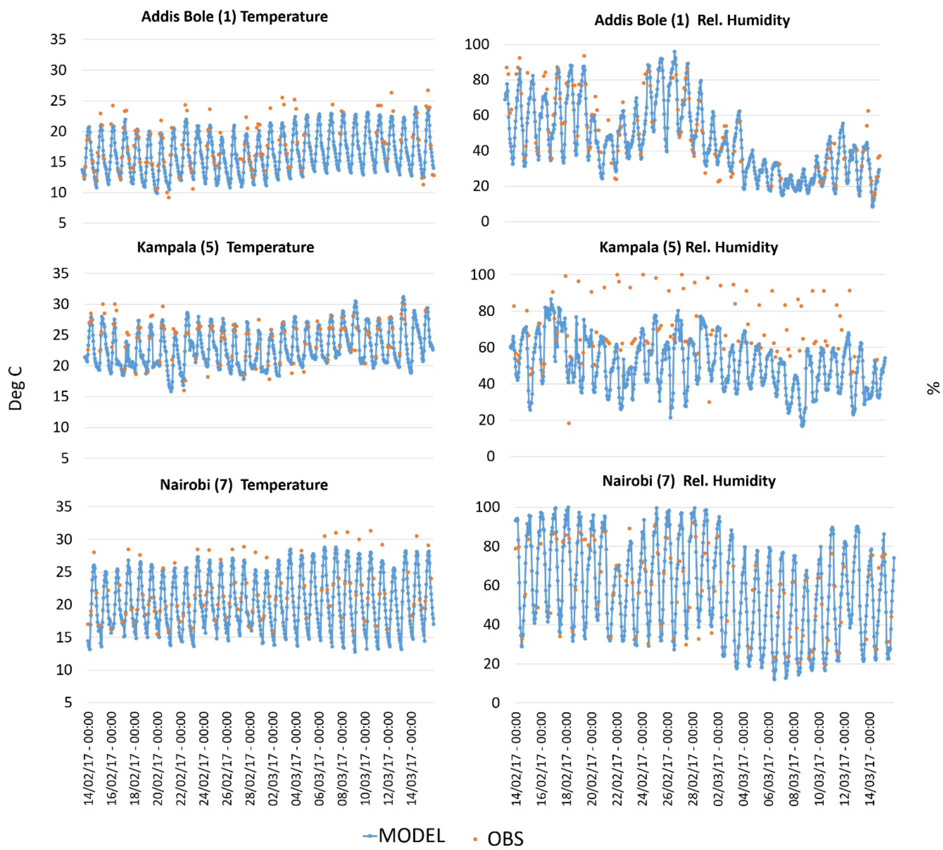

Figure 4: *Hourly time series of surface temperature (left column) and relative humidity (right column) for the closest ground weather stations to the urban centres of the cities of Addis Ababa (station 1 in Figure 3a), Kampala (station 5 in Figure 3b) and Nairobi (station 7 in Figure 3c). Comparison between modelled values (blue lines) obtained from the 2×2km domains and hourly observations (orange spots) from MIDAS database.*

The mean relative humidity observed at the three stations shows different ranges of excursion from the model predictions depending on the characteristics of the environment. The station of Addis-Bole shows the higher variation from 15 to 98 %, Nairobi station from 17 to 98 % and Kampala from 19 to 99 %. From Figure 4, it may be seen that relative humidity variations over time are correctly captured by WRF for the Nairobi and Addis-Bole stations. Both the diurnal peaks as the night lowest values seems to be correctly reproduced by the model with a mean bias between -0.1 and 0.004. However, WRF appears systematically to underestimate the relative humidity for the Kampala station showing a mean negative bias. Different reasons could affect the underestimation of the relative humidity at this station. The sensitivity of WRF model to the land use data (Teklay et al., 2019) connected with the proximity of Kampala to Lake Victoria, which is a massive inland body of water (surface area 68 800 km^2) could influence the local variation of relative humidity in ways which are not well reproduced by the model.

https://doi.org/10.5194/acp-2021-552
Preprint. Discussion started: 5 January 2022

Atmospheric Chemistry and Physics Discussions
Open Access
EGU

The influence of Lake Victoria and of the Kampala's complex topography on measurements of RH was previously highlighted by Singh et al. (2020) in relation to monthly visibility connected with PM levels. Noting that relative humidity was calculated from surface temperature and dew point values following Alduchov O. (1996) and not directly sampled, a better agreement in the simulation of relative humidity from WRF can be found in the station of Entebbe (n.4 in Figure 3b) where the mean normalized bias shows a small underestimation of 0.04 %.

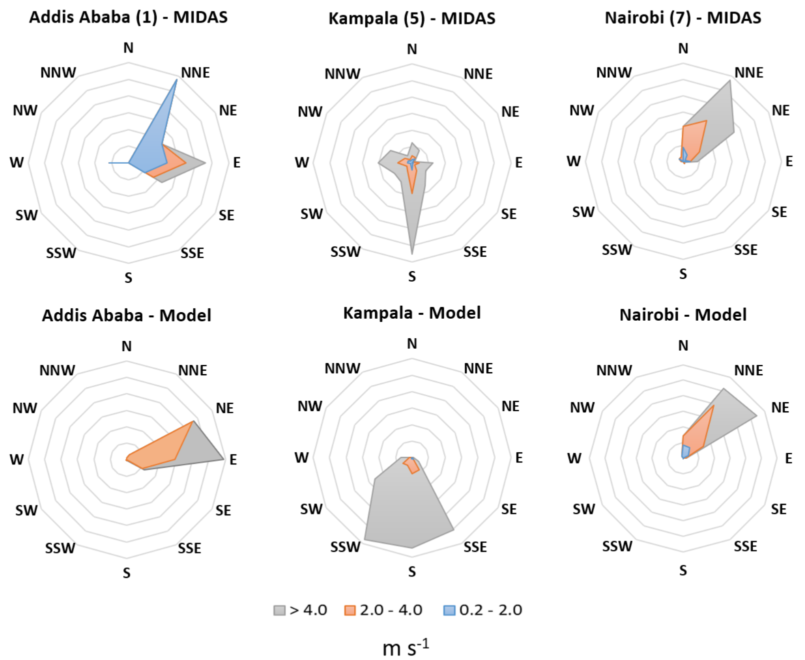

Figure 5: *Averaged wind roses for the whole analysed period (14th of February to 14th of March 2017) from the closest ground weather stations to the urban centres of Nairobi (n.7 in Figure 3c), Kampala (n.5 in Figure 3b) and Addis Ababa (n.1 in Figure 3a) (MIDAS, top) and from WRF simulation outputs (Model, bottom).*

Wind speed and directions from the urban stations of Addis-Bole (n 1 in Figure 3a), Kampala Station (n 5 in Figure 3b) and Nairobi (n 7 in Figure 3c) are shown in Figure 5 in the form of wind roses. WRF can reproduce the average wind directions in close agreement with the observed data for both sampling sites for the analysed period for Nairobi showing the predominance presence of North-North-Eastern winds with high speed (> 4.0 m s^{-1}). Moreover, the model replicates the wind directions for Nairobi and Kampala with higher agreement in comparison to Addis Ababa. The reason for this difference is due to the different locations of sampling sites that, in the case of Nairobi and Kampala are coincident with the respective airports while the wind speed and directions from Addis Ababa are relative to an urban weather station.

WRF does not appear to reproduce the wind speed and directions for Kampala as well as it does for the other two cities. For the wind speed, the observations from the ground weather stations suggest a strong southern wind

https://doi.org/10.5194/acp-2021-552
Preprint. Discussion started: 5 January 2022

component (> 4.0 m s^{-1}) while the model seems to reproduce a similar magnitude of the wind speed on a larger range of directions ranging from the South-South-East direction to South-South-West. A similar comparison between the wind roses for the city of Addis Ababa, shows that WRF is able to capture and reproduce the main wind directions observed at both observation sites for the simulated period, i.e. Eastern and North-Eastern winds. On the other hand, lower winds between 0.2 and 2.0 m s^{-1} with a strong North-North East component do not seem to be replicated by the model. Also, in this case we recall that the station of Addis-Bole is the only one settled inside an urban area, while the stations of Kampala and Nairobi are settled in the respective airports located in peri-urban areas.

The results obtained from the validation of the meteorological simulations performed over East African domains using WRF show an acceptable agreement between modelled parameters of all four variables taken in account in comparison with available observed data from the analysis done on all the averaged stations present in the 2x2 km domains. The highest agreement in the weather analysis has been found for surface temperature with similar biases to Kerandi et al. (2017) and relative humidity similar to Pohl et al. (2011), which is sufficiently accurate to be able to accurately use the physical calculations done by the chemistry transport model.

However, the more detailed analysis of the urban weather stations revealed discrepancies in the reproduction of relative humidity and wind direction for the station of Kampala (UGA2K) that could affect the deposition, removal and transport processes simulated by CHIMERE and will be object of future investigation to further improve the meteorological performance of WRF. However, for the purposes of the present work the range of bias found for the meteorological variables can be considered acceptable and the differences negligible.

3.2 Validation of CHIMERE simulations

The reliability of a chemistry-transport model needs to be evaluated against observations to quantify its confidence as air quality tool for policy making, replicating scenarios and analysis purposes. While ozone modelling and evaluation has been fairly well developed over a number of decades, with the EPA (1991) criteria still used to evaluate the level of confidence of a modelling system, for the PM evaluation the criteria used for the analysis of the performance of a modelling system are still evolving (Boylan and Russell, 2006).

One cause of uncertainty when comparing modelling outputs with observations is the difference between a point measurement and a volumetric grid cell averaged modelled concentration (Seinfeld, 2016). On one hand, the extent of a measurement point, in fact, represents only the extent of the nearby points or an average concentration in a specified area. On the other hand, a surface level modelling grid typically has a highest resolution of 1 km with a vertical height of between 20 and 40 m and the concentration represented by the model is the average over the entire grid cell.

The CHIMERE validation has been focused on the hourly levels of $PM_{2.5}$ modelled at the two observation sites for the domain KEN2K, representative of an urban roadside site and a rural background site. Also, from the urban background observational sites of the US Embassies of Kampala (UGA2K) and Addis Ababa (ETH2K). The analysis is presented in form of statistical parameters of mean normalized bias (MNB), normalized root means square error (NRMSE) and Pearson's coefficient (R) for the four observational sites on hourly and daily bases for the whole period of the simulation. The performance of CHIMERE has been analysed also in terms of mean fractional error (MFE) and mean fractional bias (MFB) against the different level of average concentrations of $PM_{2.5}$ in the four observation points to evaluate the response of the model in reproducing low and high levels of hourly concentrations in comparison with observed values.

3.2.1 Statistical evaluation of model performances

Mean observed and modelled hourly concentrations of $PM_{2.5}$ are overestimated by the model for the domain KEN2K by between 0.01 and 3.6 µg m^{-3} for Nanyuki and Nairobi, respectively, and for Addis Ababa (0.6 µg m^{-3}). On the contrary, the model underestimates $PM_{2.5}$ for the domain UGA2K (Kampala) by 7.2 µg m^{-3}. At a daily resolution, the difference between mean observed and modelled values show a similar overestimation for the two KEN2K sites, of between 0.01 and 3.8 µg m^{-3} and for Addis Ababa of 0.2 µg m^{-3} and an underestimation for Kampala of 6.7 µg m^{-3} (Table 4).

The MNB values for KEN2K suggest that, at the hourly and daily level, CHIMERE overestimates $PM_{2.5}$ values both at the roadside (i.e. MNB = 0.22 and 0.21 for hourly and daily, respectively) and at the rural sites (MNB = 0.064 and 0.062 for hourly and daily, respectively) (Table 4). In the two urban background sites of Addis Ababa and Kampala the MNB ranges between 0.88 and 0.10, and between -0.23 and -0.14, at the hourly and daily levels respectively. Hourly NRMSE values show the smallest error in the rural site of Nanyuki (0.0007) and a similar error of between 0.03 and 0.04 at the other three sites. Daily NMRSE follows the same trend with highest confidence of the model in Nanyuki (0.0011) and Nairobi (0.05) and a higher error of between 0.30 and 0.46 for Addis Ababa and Kampala, respectively.

The highest Pearson's coefficients (R) were found in Nanyuki with hourly and daily values of between 0.91 and 0.93. The roadside site of Tom Mboya street in Nairobi had R values of between 0.35 and 0.38 while the urban background sites of Addis Ababa and Kampala had a lower agreement an hourly level (R values were between 0.10 and 0.29, respectively) than at a daily level (R values of between 0.42 and 0.30, respectively).

In general, the statistical analysis described above demonstrates that the model can reproduce satisfactorily the daily pattern of the hourly changes in concentrations for the two pollutants both in the three urban sites and in the rural site considered. The low R coefficient values obtained for the urban domains at the hourly level suggests that sources of anthropogenic emissions affecting urban air quality are missing from the current emission inventory. Further work will be focused on the improvement of the magnitude of the emissions to better match the observed levels of concentrations of particulate matter at the urban level. Despite this and considering the daily average concentrations in the urban sites, the R coefficients were found to be between 30 and 42 % suggesting that CHIMERE better reproduces the concentrations of $PM_{2.5}$ using daily averaging.

https://doi.org/10.5194/acp-2021-552
Preprint. Discussion started: 5 January 2022

Table 4: *Hourly and daily statistical evaluation of CHIMERE model performance for the cities of Nairobi against ASAP observed data and against US Embassies data for the cities of Addis Ababa and Kampala*

ASAP OBS	**NAIROBI $PM_{2.5}$ (roadside)**		**NANYUKI $PM_{2.5}$ (rural)**	
	DAILY	**HOURLY**	**DAILY**	**HOURLY**
Mean MOD	58.33	58.16	3.24	3.24
Mean OBS	54.58	54.57	3.23	3.23
MNB	0.21	0.22	0.062	0.064
NRMSE	0.05	0.03	0.0011	0.0007
R	0.38	0.35	0.93	0.91
U.S. EMBASSY OBS	**ADDIS A. – $PM_{2.5}$ (urban)**		**KAMPALA – $PM_{2.5}$ (urban)**	
	DAILY	**HOURLY**	**DAILY**	**HOURLY**
Mean MOD	18.6	18.7	36.2	36.2
Mean OBS	18.4	18.1	42.9	43.4
MNB	0.10	0.88	-0.14	-0.23
NRMSE	0.30	0.03	0.46	0.04
R	0.42	0.10	0.30	0.29

3.2.2 Mean Fractional Bias evaluation

MFB and MFE normalise the bias and the error for each model-observed pair by the average of the model and observation before taking the final average (Eq. 2 and 3). The advantage of these metrics is that the maximum bias and errors are bounded, and that impact of outlier data points are minimised. Moreover, the metrics are symmetric giving equal weight, to concentrations simulated higher than observations and to those that are simulated lower than observations.

$$MFB = \frac{1}{N}\sum_{i=1}^{N}(C_m - C_o)/(C_o + C_m/2) \quad \text{Eq. (2)}$$

$$MFE = \frac{1}{N}\sum_{i=1}^{N}|C_m - C_o|/(C_o + C_m/2) \quad \text{Eq. (3)}$$

MFB and MFE have been expressed in terms of model performance goals and model performance criteria values according to the methodology proposed by Boylan and Russell (2006). The performance goal for the modelling system is attested for MFE ≤ 50% and MFB ≤ ± 30%. In this range of values (shown as green dashed lines in Figure 6) the performance of the model in reproducing the correct magnitude of the concentrations can be considered good. A second larger range of values, called criteria, is attributed for MFE ≤ 75% and MFB ≤ ± 60%. Values inside this are (shown as red dashed lines in Figure 6) corresponds to an average model performance. Finally values with MFE > 75% and -60% > MFB > +60% represent a poor representation by the model.

https://doi.org/10.5194/acp-2021-552
Preprint. Discussion started: 5 January 2022

Table 5: *Hourly mean fractional bias (MFB) and error (MFE) percentage of points inside the goal limit (GOAL), inside the diagnostic range (CRITERIA) and outside the reliability criteria (OUT) from model outputs extracted from the four analysed locations.*

City	MFB			MFE		
	GOAL (%)	CRITERIA (%)	OUT (%)	GOAL (%)	CRITERIA (%)	OUT (%)
Tom Mboya St. (KEN2K)	69	22	9	88	7	5
Nanyuki (KEN2K)	97	2	1	99	1	0
Kampala (UGA2K)	48	37	15	74	16	10
A.Ababa (ETH2K)	57	30	13	80	11	9

The MFB and MFE analysis has been conducted comparing modelling outputs and observations from Nairobi and Nanyuki in KEN2K, and from the US Embassies of Kampala and Addis Ababa. The model performance in reproducing the $PM_{2.5}$ for the two sites in KEN2K shows a higher percentage of values within the MFB and MFE performance goals for the rural site of Nanyuki, than for Tom Mboya Street. i.e. 97% compared to 69% and 99% compared to 88% for the MFB and MFE measures respectively. For the criteria measure, the corresponding percentages are 2% vs. 22% and 1 vs. 7%.

The percentages for the urban sites of Kampala and Addis Ababa show a lower agreement between the model and observations. For the former 48 % of the values according to the MFB measure are within the goal range, 37% are within the criteria range and 15 % are outside. For the latter, according to the MFB criteria, 57 % of the values are inside the goal range, 30 % of values are within the criteria range and 13 % are outside. In terms of the MFE measure, 74 % and 80 % of values for the two cities are within the goal range, 16 % and 11 % within the criteria range and 10 % and 9 % outside respectively.

According to the methodology proposed by (Boylan and Russel, 2006) the performance of a modelling system is fairly good for $PM_{2.5}$ representation if about the 50 % of the points are within the goal range and a large majority are within the criteria range. From the analysis of the four sampling sites the values of MFB inside both the goal and range for Tom Mboya street are 69%, 97% for Nanyuki and 57% for Addis Ababa and only for Kampala are 48 %. Similarly, for the MFE measure, 99 % for Nanyuki, 88 % for Tom Mboya street, 80 % for Addis Ababa and 74 % for Kampala are inside both the goal range. The demonstrates that the performance of the model can be considered to be satisfactory.

https://doi.org/10.5194/acp-2021-552
Preprint. Discussion started: 5 January 2022

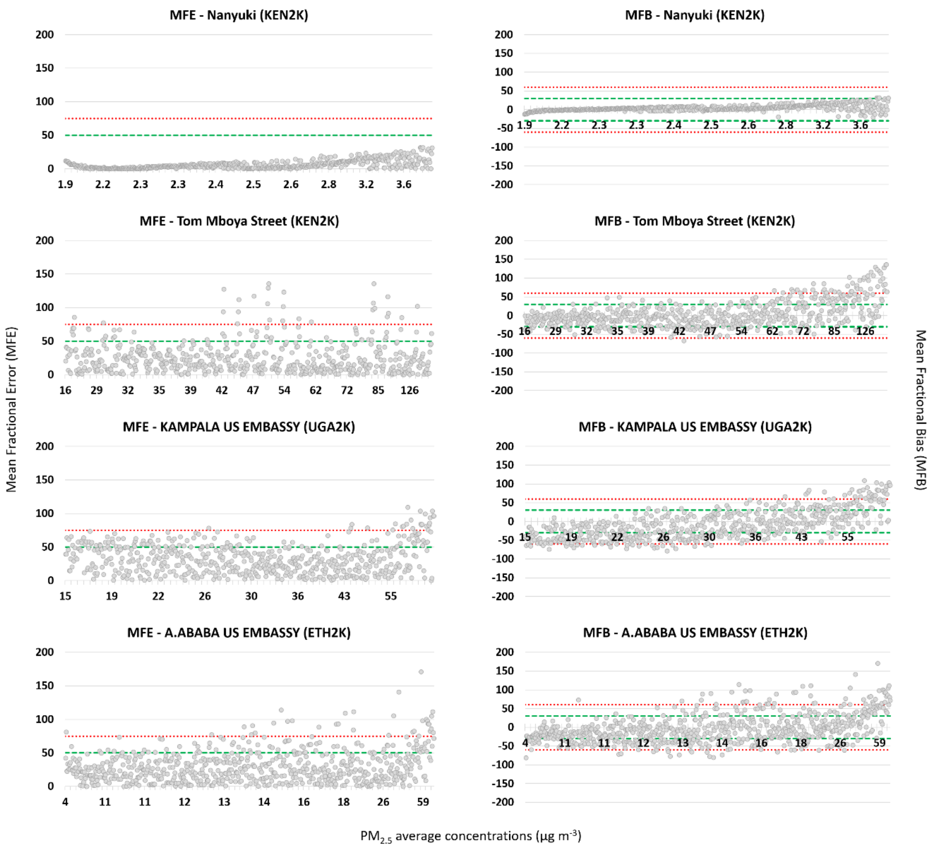

Figure 6: *Hourly mean fractional bias (MFB) and mean fractional error (MFE) values calculated for the locations of Tom Mboya Street and Nanyuki (KEN2K), Kampala US Embassy (UGA2K) and Addis Ababa US Embassy (ETH2K) for the analysed period against hourly concentrations of $PM_{2.5}$. The green lines represent the MFB range ±30µg m^{-3} and the MFE limit of 50 µg m^{-3} for which the model performance can considered reliable, the red lines represent the MFB range ±60 µg m^{-3} and the MFE limit of 75 µg m^{-3} for which model performance can be increased by diagnostic analysis on the chemical precursors of $PM_{2.5}$.*

There are some MFB values outside the criteria range for $PM_{2.5}$ for the urban sites of Addis Ababa and Kampala and for the roadside site of Tom Mboya Street in Nairobi. In terms of the upper limit (MFB > 60%) these values tend to be concentrated between 60 and 130 µg m^{-3} for Tom Mboya street, 40 and 55 µg m^{-3} for Kampala and between 13 and 59 µg m^{-3} for Addis Ababa (Figure 6). A much smaller number of MFB values for the Addis Ababa and Kampala sites are less than the lower criteria limit and these tend to be for lower concentrations between 10 and 26 µg m^{-3}.

MFE values outside the ranges of criteria are between 42-55 and 80-130 µg m^{-3} for Tom Mboya street, 43 and 60 µg m^{-3} for Kampala and 13 and 59 µg m^{-3} for Addis Ababa (Figure 6). The latter two sites present a more variability of MFB and MFE in comparison with the two sites of Kenya where is visible a common positive bias of the model in reproducing the highest concentration levels. The reliability of the model is therefore higher for the domain of

Kenya, both for a rural and for a roadside site than for the two urban background sites in Uganda and Ethiopia. The reason for the presence in the Addis Ababa and Kampala simulations of values outside the criteria range both at high and at low concentrations of $PM_{2.5}$ can be connected to the representation of the original PM emissions in the combined inventory and their representation and chemical reactivity inside CHIMERE that does not correctly reproduce all the chemical processes involved in the formation of inorganic and organic individual components of $PM_{2.5}$. Moreover, the possible misrepresentation of local emission sources not reproduced in DICE-EDGAR can also affect the performance of the model. Finally, the different location of the urban background observation sites and the sampling techniques for PM observation can also have a key role in the correct detection of the concentrations.

3.2.3 Hourly variation of $PM_{2.5}$ in urban and rural sites of Kenya

Hourly modelled variation of $PM_{2.5}$ levels obtained by CHIMERE compared with observations from the field are shown for the urban sampling site of Tom Mboya Street, Nairobi and for the rural site of Nanyuki (Figure 7). By inspection of Figure 7 it can be seen that CHIMERE is able, in general, to reproduce the daily variation of $PM_{2.5}$ across the simulated period at both sites.

The magnitude of the emissions adopted seems to be suitable both for the roadside area of Tom Mboya street and for the rural background site of Nanyuki, with higher agreement shown by the latter. CHIMERE captures only part of the daily peak observed in Tom Mboya Street with comparable magnitude but misrepresents some peaks. In particular it models higher hourly peaks than those observed as previously mentioned in the MFB and MFE analysis above (Figure 8).

The misrepresentation of some high peaks in Tom Mboya street is possibly due to a number of different reasons. Firstly, is important to recall that the point measurements and relative observed concentrations are representative of a smaller portion of space in comparison with grid-cell concentrations modelled. In this particular case the comparison is between a roadside site subjected to possible additional local sources of $PM_{2.5}$ not accounted for in the emissions and not correctly reproduced by CHIMERE. On the other hand, a few of the modelled peaks results were overestimated. This can be addressed by improved temporal description of the input emissions and in their magnitude in comparison to the reality. As mentioned previously, the anthropogenic emissions used in this work were the most up-to-date available at the time and that there is inevitably some difference between the measured data due to the difference in time between the inventories and the measurements. Despite this, there is reasonable agreement between model outputs and observed concentrations for the majority of the analysed period highlighting the reliability of CHIMERE in describing the hourly concentrations trends for a roadside site with expected high levels of $PM_{2.5}$ contamination.

https://doi.org/10.5194/acp-2021-552
Preprint. Discussion started: 5 January 2022

Atmospheric Chemistry and Physics Discussions
Open Access
EGU

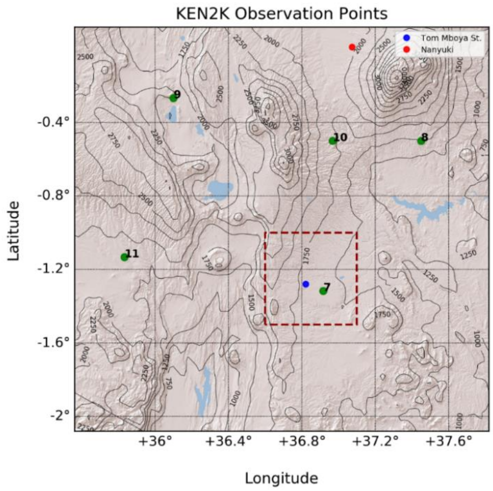

Figure 7: *Map showing the second nested domain used in CHIMERE to simulate $PM_{2.5}$ concentrations over Kenya. The blue dot shows the location of the roadside site of Tom Mboya Street in Nairobi (1.28°S, 36.82°E) while the red dot shows the location of the rural site of Nanyuki (0.01°N, 37.07°E). The green dots show the locations of all the MIDAS weather stations listed in Table 2 while the red dashed square defines the area of Nairobi. The contour lines represent the topography from the WRF outputs.*

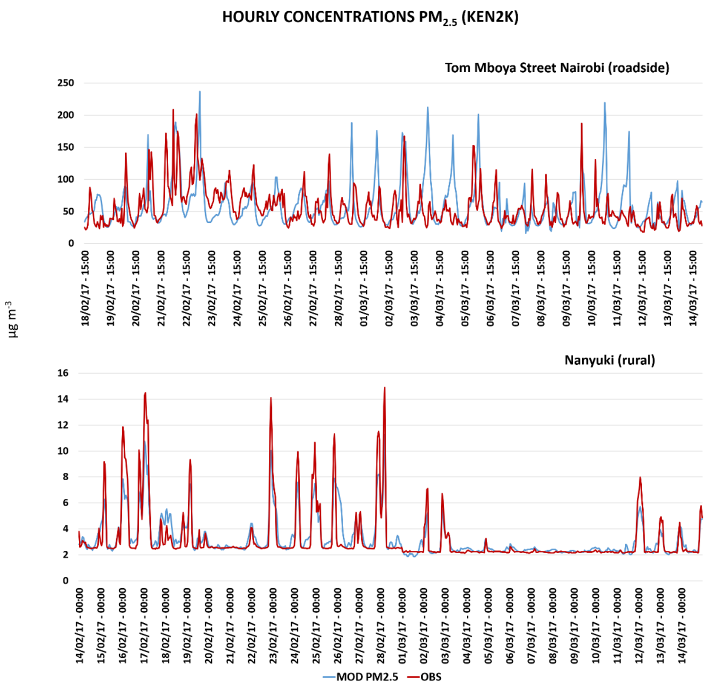

Figure 8: *Hourly time series for $PM_{2.5}$ from the roadside of Tom Mboya Street (top) and from the rural site of Nanyuki (bottom) from modelled output from CHIMERE model (blue line) and observed values from Pope et al. (2018) (red line) for the analysed period The simulation started on the 14th of February. For the Tom Mboya Street site only the period of time between the 18th of February and the 14th of March when observations were available has been shown in the timeseries.*

https://doi.org/10.5194/acp-2021-552
Preprint. Discussion started: 5 January 2022

Atmospheric Chemistry and Physics Discussions

Similarly, in the rural site of Nanyuki, the model seems to correctly reproduce the hourly variation of the concentrations during the whole period, underestimating the maximum peaks at the beginning of February and in the last four days of simulation in March. (Figure 8). The site shows different magnitudes in the concentrations of $PM_{2.5}$ when comparing the February and March periods. While between the 4th and the 10th of March hourly concentrations are around 3-4 µg m^{-3}, previously and subsequently to this period of time, the concentrations of $PM_{2.5}$ are more than two times higher. This behaviour is visible both in the observations from the site (red line in Figure 8, bottom) and from the model outputs obtained using CHIMERE (blue line in Figure 8, bottom).

A possible reason for this different behaviour may be due to different weather conditions of wind speed and wind directions during February and March in that particular area. The closest MIDAS weather station to the sampling area of Nanyuki is in the town of Nyeri (0.43°N, 36.95°E altitude 1916 m a.g.l.) (n 10 in Figure 7). Nyeri is only 60 km from the Nanyuki site and is situated between Mount Kenya (0.10°N, 37.30°E, altitude 4341 m a.g.l.) to the west and the Aberdare Range (0.46°N, 36.69°E, altitude 3441 m a.g.l.).

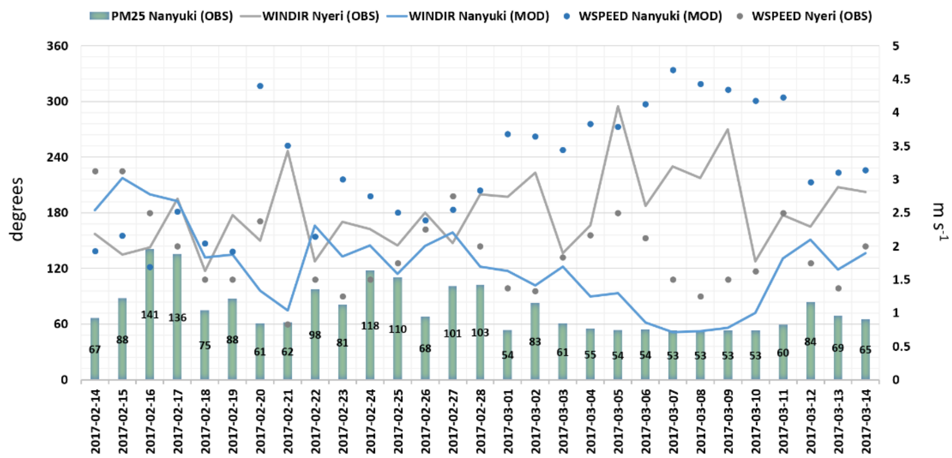

Figure9: *Comparison between daily observed values of wind speed (grey dots) directions (grey lines) from the MIDAS site of Nyeri (n.10 in Figure 7), modelled daily wind speed (blue dots) and directions (blue lines) from the site of Nanyuki with daily total observations of $PM_{2.5}$ (expressed in µg m^{-3} , green columns) obtained from the sampling site of Nanyuki (red dot in Figure 7).*

The daily total concentrations observed in the sampling site of Nanyuki have been compared with the daily mean values of wind speed and directions observed at the MIDAS station of Nyeri and with the daily mean values of wind speed and directions modelled by WRF in Nanyuki (Figure 9). The period between the 4th and the 10th of March, when the daily total $PM_{2.5}$ observed in Nanyuki was around 55 µg m^{-3} corresponds to higher wind speed conditions (between 4 and 5 m s^{-1}) mainly coming from North-Est (around 60 degrees). In the same period, at Nyeri the modelled wind speed was low (between 1 and 2.5 m s^{-1}) and mainly with a westerly component (between 220 and 300 degrees).

https://doi.org/10.5194/acp-2021-552
Preprint. Discussion started: 5 January 2022

Atmospheric Chemistry and Physics Discussions

In the periods of higher hourly concentrations of $PM_{2.5}$ between the 15th and the 19th and between 22nd and the 28th of February 2017, both in Nyeri (using observations) and in Nanyuki (using model outputs) the component of wind directions seems to be consistent in reproducing southern winds (between 120 and 190 degrees) with wind speeds between 1.5 and 2.5 m $^{-s}$ in the first period and between 2 and 3 m^{-s} in the second period.

The correspondence between the wind speed and directions in particular time periods and the vicinity of the towns could suggest the potential dispersion of pollutants from the southern area of Nyeri to the northern area of Nanyuki in accordance with the wind fluxes from south to north from Nyeri from the observations and also from WRF outputs extracted from the Nanyuki location. The flux could also be driven by the location of Nyeri sited at the entrance of a basin between two mountain ranges. On the other hand, in the period of low concentrations between the 4th and the 10th of March north eastern winds (around 60 degrees) blow with high speed on Nanyuki (around 4 m s^{-2}) while lower speed winds (between 1 and 2 m s^{-2}) from a more variable directions (between 170 and 300 degrees) are apparent in Nyeri preventing the possible dispersion of pollutants.

This evaluation done on the relationships between weather conditions and the relative correspondence in hourly and daily levels of $PM_{2.5}$ cannot exclude the presence of possible transport phenomena. Nevertheless, the lack of additional weather observations in the sampling site of Nanyuki and in the middle way between the two towns prevent from any additional hypothesis in relation to the presence of possible pollutant transport phenomena that will be object of future investigations. Further efforts will be oriented in a more detailed trajectory analysis of the winds and in a more detailed representation of the emissive sources present in the area to investigate possible transport effects in this area.

3.3 CHIMERE as an Air Quality Management Tool

The usefulness of CHIMERE as a decision support tool to facilitate air quality management of large urban conurbations of SSEA was investigated for the three domains at a resolution of 2×2 km, namely: KEN2K, UGA2K and ETH2K. In order to evaluate the performance of CHIMERE as a decision support tool, daily observations of $PM_{2.5}$ for the three domains were compared with modelled concentrations in terms of number of exceedances from the WHO limit of 25 µg m^{-3} observed and captured by the model (Figure 10). Moreover, for the case of Nairobi, the spatial distribution of daily average concentrations of $PM_{2.5}$ on the constituencies where analysed, highlighting how many areas of the city showed low air quality indexes during the analysed period and the relative population density exposed to $PM_{2.5}$ pollution (Figure 11).

https://doi.org/10.5194/acp-2021-552
Preprint. Discussion started: 5 January 2022

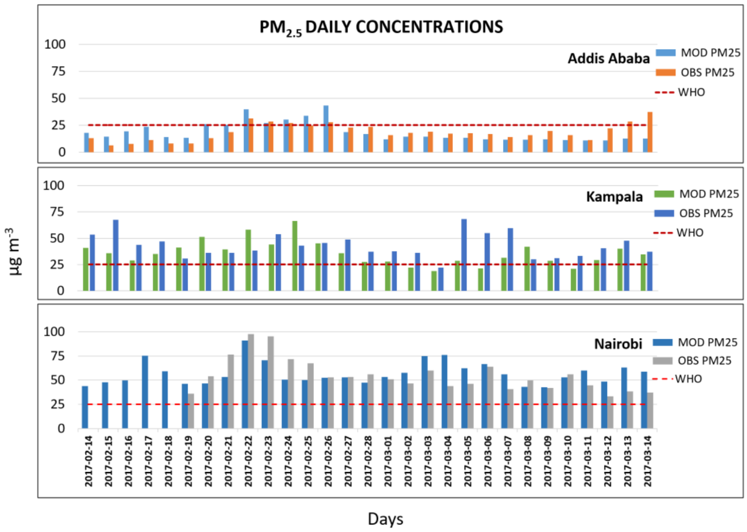

Figure 10: *Daily concentrations of $PM_{2.5}$ between the 14th of February and 14th of March obtained from CHIMERE outputs from domains at 2x2 km compared with US Embassy daily totals for the cities of Addis Ababa (top) and Kampala (middles) and with ASAP observations for the city of Nairobi (bottom). All three simulations have been compared also with the WHO threshold limit for $PM_{2.5}$ concentrations (red line). For the case of Nairobi, only observations from the 18th of February were available.*

Daily concentrations of $PM_{2.5}$ modelled by CHIMERE were compared with the number of exceedances of the WHO limit (i.e. 25 µg m^{-3}) observed during the simulated period. Figure 10 shows the daily average concentrations for the three cities in the sampling sites used for the validation of the model. It can be seen that Nairobi and Kampala have the highest number of exceedances from the WHO limits (24) followed by Addis Ababa with only 6 observed exceedances. From Table 6 it can be seen that CHIMERE provides sufficient accuracy to detect the exceedances of $PM_{2.5}$ from the WHO limits. In particular, it was able to detect 67 % of the exceedance for Addis Ababa with only two false positives, 91 % for Kampala and all of the exceedances for Nairobi without any false positives.

Table 6: *Summary of the number of WHO exceeding limits for $PM_{2.5}$ during the simulated period from the 14th of February to the 14th of March 2017 observed and modelled. Ratio between the observed and modelled Exceeding limit and number of model overestimations are also reported.*

Domains	WHO Exceeding Limits (obs)	WHO Exceeding Limits (mod)	Ratio (%)	Model False positive
Nairobi	24	24	100	0
Addis Ababa	6	4	67	2
Kampala	24	22	91	0

The Air Quality Index (AQI) represents the conversion of concentrations for fine particles such as $PM_{2.5}$ to a number on a scale from 0 to 500 (Table 7). The higher the AQI value, the greater the level of air pollution and the greater the health concern. AQI values at or below 100 are generally thought of as satisfactory. When AQI values are above 100, air quality is unhealthy: at first for certain sensitive groups of people (101 – 150), then for everyone as AQI values get higher (>151) (EPA, 2012).

https://doi.org/10.5194/acp-2021-552
Preprint. Discussion started: 5 January 2022

Atmospheric Chemistry and Physics Discussions
Open Access
EGU

The daily average concentrations of $PM_{2.5}$ during the analysed period between the 14th of February and 15th of March 2017 have been averaged for the urban area of Nairobi (red square in Figure 7) and compared with the city constituencies spatial extension according to data from the Open Africa dataset (Open-Africa, 2018). According to the division, 17 are the constituencies inside the Nairobi city boundaries (Figure 11). Averaged daily concentrations of $PM_{2.5}$ show that 8 of 17 constituencies had AQI values between 55.5 - 150.4 µg m^3 during the whole period. These areas are the most central and urbanized of Nairobi. Starehe constituency (n. 13 in Figure 11) contains the Tom Mboya Street sampling site (black spot in Figure 11) previously discussed where the WHO limits for $PM_{2.5}$ have been systematically exceeded during the analysed period. According to the SEDAC population density data this area has population density between 15000 and 30000 people/km^2 exposed to AQI between 151-200 corresponding to unhealthy category for human health.

Table 7: *Air Quality Index categories and relative range of 24-hour average concentrations for $PM_{2.5}$ reported by the US EPA revised air quality standard for particle pollution of 2012 (EPA, 2012)*

AQI Category	Index values	AQI Breakpoints (µg m^{-3} on 24-hour average)
Good	0 - 50	0.0 - 12.0
Moderate	51 - 100	12.1 - 35.4
Unhealthy for sensitive Groups	101 - 150	35.5 - 55.4
Unhealthy	151 - 200	55.5 - 150.4
Very Unhealthy	201 - 300	150.5 - 250.4
Hazardous	>301	>250.5

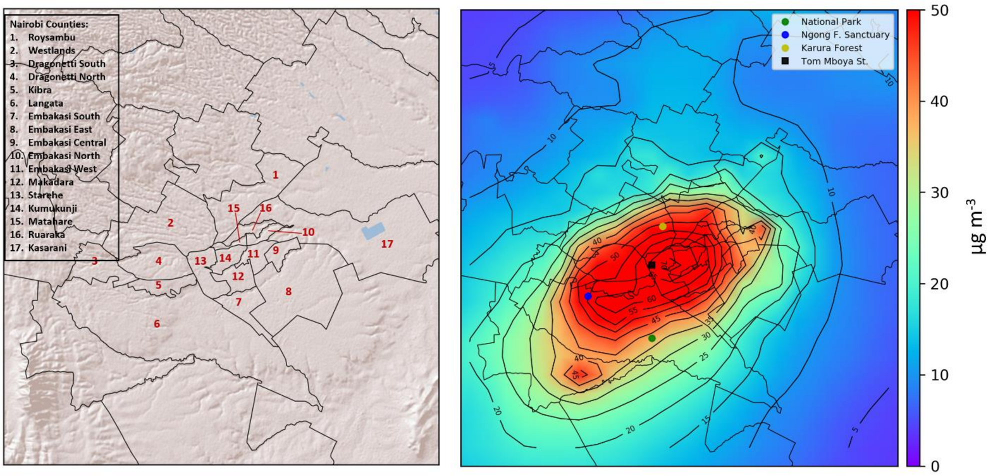

Figure 11: *Map showing the urban area of the city of Nairobi shown as dashed square in Figure 7. The constituency division of Nairobi (left image)from Open Africa dataset (Open Africa, 2018) is compared with the average hourly concentrations of $PM_{2.5}$ over the analysed period (top right) and the corresponding Air Quality Index levels as reported by the US EPA revised air quality standard for particle pollution of 2012 (bottom right) (EPA, 2012) .*

https://doi.org/10.5194/acp-2021-552
Preprint. Discussion started: 5 January 2022

Atmospheric Chemistry and Physics Discussions

Moreover, Nairobi has a number of natural areas on the outskirts of city. Some particular locations such as the Karura Forest (yellow spot in Figure 11) and the Ngong Forest Sanctuary (blue spot in Figure 11) show averaged daily levels of $PM_{2.5}$ around 50 and 55 µg m^3 corresponding to an AQI of between 101 and 150 (i.e. unhealthy for certain sensitive groups of people). According to SEDAC data, the population density is between 10000 and 15000 people for km^2 in this area. Similarly, in the south side, near the entrance to the Nairobi National Park (1.36° S, 36.82° E, green spot in Figure 10) the average daily levels of $PM_{2.5}$ are approximately 40 µg m^3 with AQI values between 101 and 150 with a population density around 10000 people for km^2. This area (surface area 117 km^2) has been impacted by a rapid urbanization since 1973 with a consequent increase of human activities including settlement, pastoralism and agriculture (Ogega O.M., 2019). These activities have already made it difficult for wildlife to migrate to and from the Nairobi National Park also are resulting in a deterioration of air quality. The rapid increase of population density in the south side of Nairobi seriously risk increasing the level or AQI exposing more people to harmful level of $PM_{2.5}$.

4 Conclusions

The coupled modelling system WRF-CHIMERE was implemented and validated to simulate the air quality levels of PM in Eastern Sub-Saharan African urban conurbations.

In order to obtain updated anthropogenic emissions for 2017, the global EDGAR inventory and the DICE inventory for Africa were merged and spatially distributed using population density data for the year 2017 obtained by linear extrapolation.

WRF has proved capable of reproducing the main meteorological patterns for all domains considered. A lower agreement between observations and the model was observed in Kampala for relative humidity and wind speed. The analysis was carried out on all surface meteorological stations available from the MIDAS network on a three-hourly basis. A further meteorological analysis extended to vertical profiles could reveal possible limitations of the model. However, the absence of vertical meteorological data limited the analysis and validation to ground level only.

CHIMERE was able to reproduce the daily levels of $PM_{2.5}$ for the urban site of Nairobi as well as for the rural site of Nanyuki. The 69 % of the MFB values and 88 % of the MFE value were inside the highest confidence area for Nairobi and the 97 % and 99 % for Nanyuki attesting that the agreement between the observed and modelled data was sufficient to allow for quantitative analyses of daily average concentrations. Similar findings were also found for the other two urban background domains of Addis Ababa (57 % for MFB and 80 % for MFE) and Kampala (48% for MFB and 74 % for MFE) despite different characteristics and sources of observation being used for the validation. The discrepancies observed in the hourly trends of $PM_{2.5}$ modelled by CHIMERE compared to observed values in the urban sites suggest that further studies are needed in the three urban areas. These studies are required to improve the understanding of the typology and quantity of local emission sources, which are sometimes misrepresented or absent in global emission inventories. This will enable the chemical processes acting in the urban troposphere to be adequately characterised and thereby actual air quality levels to be determined.

https://doi.org/10.5194/acp-2021-552
Preprint. Discussion started: 5 January 2022

Atmospheric Chemistry and Physics Discussions

Nevertheless, using existing data sets, CHIMERE has shown reliability in reproducing both hourly and daily levels of $PM_{2.5}$ with hourly values largely inside the range of reliability connected with mean fractional bias and error. The model therefore can be adopted as a decision support tool for the management of air quality, as despite the low resolution of anthropogenic emissions the model can reproduce most of the exceedances of the limits set by the WHO for $PM_{2.5}$ for all three cities considered. The work has also shown for Nairobi the presence of low and unhealthy air quality indexes in 8 of 17 its constituencies and the relative population density exposed to harmful level of air contamination. Moreover, a number of natural areas in the outskirts of Nairobi have similarly low levels of AQI and increasing population highlighting how the problem of poor urban air quality due to rapid urbanisation, anthropogenic activities and lack of regulation can also detrimentally affect and deteriorate natural habitats.

Future efforts to improve the calibration and validation of the modelling system, especially relating to meteorology, will focus on assessing the dispersion dynamics of contaminants through urban centres and possible pollution transport events from urban to rural areas. To aid this, further work is required by local East African authorities and research bodies to improve the quantity and the quality of data for weather and air quality simulations. However, in this work, we have shown that currently available data is sufficient to carry out simulations of air quality that can be used for quantitative evaluation of anthropogenic emissions impact and to support mitigation policies at the local level.

Authors Contribution: Andrea Mazzeo: Conceptualization, Methodology, Software, Validation, Writing- Original draft preparation, Writing- Reviewing and Editing. **Michael Burrow:** Supervision, Writing - Review & Editing **Andrew Quinn:** Supervision, Resources. **Eloise A. Marais**: Data curation, Resources, Writing - Review and Editing. **Ajit Singh**: Resources, **David N'gang'a:** Resources, **Michael Gatari:** Resources. **Francis Pope**: Supervision, Data curation, Funding acquisition.

Acknowledgements:
The work is funded by the UK Department for International Development (DFID) via the EPSRC grant 'Digital Air Quality' (EP/T030100/1) and by the East Africa Research Fund (EARF) grant 'A Systems Approach to Air Pollution (ASAP) East Africa'. The practical support of the Schools of Geography and Earth Sciences and Engineering at the University of Birmingham are gratefully acknowledged.

Data Availability: the combined DICE-EDGAR anthropogenic emission inventory is downloadable from: https://doi.org/10.25500/edata.bham.00000695

References

Alduchov O., E. R.: Improved Magnus Form Approximation of Saturation Vapor Pressure, J. Of Appl. Met., 35, 601-609, https://doi.org/10.1175/1520-0450(1996)035<0601:IMFAOS>2.0.CO;2,, 1996.

Amegah, A. K., and Agyei-Mensah, S.: Urban air pollution in Sub-Saharan Africa: Time for action, Environ Pollut, 220, 738-743, 10.1016/j.envpol.2016.09.042, 2017.

https://doi.org/10.5194/acp-2021-552
Preprint. Discussion started: 5 January 2022

Atmospheric Chemistry and Physics Discussions
Open Access EGU

Anav, A., Menut, L., Khvorostyanov, D., and VİOvy, N.: Impact of tropospheric ozone on the Euro-Mediterranean vegetation, Global Change Biology, 17, 2342-2359, 10.1111/j.1365-2486.2010.02387.x, 2011.

Assamoi, E.-M., and Liousse, C.: A new inventory for two-wheel vehicle emissions in West Africa for 2002, Atmospheric Environment, 44, 3985-3996, 10.1016/j.atmosenv.2010.06.048, 2010.

Avis W. and Khaemba W.: Vulnerability and air pollution, 2018.

Barnard, J.: An evaluation of the FAST-J photolysis algorithm for predicting nitrogen dioxide photolysis rates under clear and cloudy sky conditions, Atmospheric Environment, 38, 3393-3403, 10.1016/j.atmosenv.2004.03.034, 2004.

Bessagnet, B., Pirovano, G., Mircea, M., Cuvelier, C., Aulinger, A., Calori, G., Ciarelli, G., Manders, A., Stern, R., Tsyro, S., García Vivanco, M., Thunis, P., Pay, M.-T., Colette, A., Couvidat, F., Meleux, F., Rouïl, L., Ung, A., Aksoyoglu, S., Baldasano, J. M., Bieser, J., Briganti, G., Cappelletti, A., D'Isidoro, M., Finardi, S., Kranenburg, R., Silibello, C., Carnevale, C., Aas, W., Dupont, J.-C., Fagerli, H., Gonzalez, L., Menut, L., Prévôt, A. S. H., Roberts, P., and White, L.: Presentation of the EURODELTA III intercomparison exercise – evaluation of the chemistry transport models' performance on criteria pollutants and joint analysis with meteorology, Atmospheric Chemistry and Physics, 16, 12667-12701, 10.5194/acp-16-12667-2016, 2016.

Bian, H., Prather, M.: Fast-J2: accurate simulation of stratospheric photolysis in global chemical models, J. Atmos. Chem, 41, 281–296, https://doi.org/10.1023/A:1014980619462, 2002.

Bockarie, A. S., Marais, E. A., and MacKenzie, A. R.: Air Pollution and Climate Forcing of the Charcoal Industry in Africa, Environ Sci Technol, 54, 13429-13438, 10.1021/acs.est.0c03754, 2020.

Boylan, J. W., and Russell, A. G.: PM and light extinction model performance metrics, goals, and criteria for three-dimensional air quality models, Atmospheric Environment, 40, 4946-4959, 10.1016/j.atmosenv.2005.09.087, 2006.

Brauer, M., Amann, M., Burnett, R. T., Cohen, A., Dentener, F., Ezzati, M., Henderson, S. B., Krzyzanowski, M., Martin, R. V., Van Dingenen, R., van Donkelaar, A., and Thurston, G. D.: Exposure assessment for estimation of the global burden of disease attributable to outdoor air pollution, Environ Sci Technol, 46, 652-660, 10.1021/es2025752, 2012.

Carter, W. P. L.: Development of the SAPRC-07 chemical mechanism, Atmospheric Environment, 44, 5324-5335, 10.1016/j.atmosenv.2010.01.026, 2010.

Collins, W., Rasch, P., Boville, B., Hack, J., McCaa, J., Williamson, D., Kiehl, J., Briegleb, B., : Description of the NCAR Community Atmosphere Model (CAM 3.0). , NCAR Tech Notes, 2004.

Crippa M., G. D., Muntean M., Shaaf E., Dentener F., van Aardenne J.A., Monni S., Doering U., Olivier J.G.J., Pagliari V. and Janssens-Maenhout G.: Gridded emissions of air pollutants for the period 1970-2012 within EDGAR v4.3.2, Earth Sci. Data, 10, 1987 – 2013, https://doi.org/10.5194/essd-2018-31, 2018.

Dalal, S., Beunza, J. J., Volmink, J., Adebamowo, C., Bajunirwe, F., Njelekela, M., Mozaffarian, D., Fawzi, W., Willett, W., Adami, H. O., and Holmes, M. D.: Non-communicable diseases in sub-Saharan Africa: what we know now, Int J Epidemiol, 40, 885-901, 10.1093/ije/dyr050, 2011.

deSouza P., N. V., Klopp J. M., Shaw B. E., Ho W. O., Saffell J., Jones R. and Ratti C.: : A Nairobi experiment in using low cost air quality monitors, Clean Air Journal, 27, 12-42, http://dx.doi.org/10.17159/2410-972X/2017/v27n2a6, 2017.

Egondi, T., Kyobutungi, C., Ng, N., Muindi, K., Oti, S., van de Vijver, S., Ettarh, R., and Rocklov, J.: Community perceptions of air pollution and related health risks in Nairobi slums, Int J Environ Res Public Health, 10, 4851-4868, 10.3390/ijerph10104851, 2013.

Guidance for regulatory application of the urban airshed model UAM, 1991.

Revised Air Quality Standards for particle pollution and updates to the Air Quality Index (AQI): https://www.epa.gov/sites/production0-etrfvgy8ufiles/2016-04/documents/2012_aqi_factsheet.pdf 2012.

Gaita, S. M., Boman, J., Gatari, M. J., Pettersson, J. B. C., and Janhäll, S.: Source apportionment and seasonal variation of PM_{2.5} in a Sub-Saharan African city: Nairobi, Kenya, Atmospheric Chemistry and Physics, 14, 9977-9991, 10.5194/acp-14-9977-2014, 2014.

Gatari, M. J., Kinney, P. L., Yan, B., Sclar, E., Volavka-Close, N., Ngo, N. S., Mwaniki Gaita, S., Law, A., Ndiba, P. K., Gachanja, A., Graeff, J., and Chillrud, S. N.: High airborne black carbon concentrations measured near roadways in Nairobi, Kenya, Transportation Research Part D: Transport and Environment, 68, 99-109, 10.1016/j.trd.2017.10.002, 2019.

Guenther, A., Karl, T., Harley, P., Wiedinmyer, C., Palmer, P., and Geron, C.: : Estimates of global terrestrial isoprene emissions using MEGAN (Model of Emissions of Gases and Aerosols from Nature), Atmos. Chem. Phys, 6, 3181–3210, https://hal.archives-ouvertes.fr/hal-00295995, 2006.

Hauglustaine, D. A., Hourdin, F., Jourdain, L., Filiberti, M. A., Walters, S., Lamarque, J. F., and Holland, E. A.: Interactive chemistry in the Laboratoire de Météorologie Dynamique general circulation model: Description and background tropospheric chemistry evaluation, Journal of Geophysical Research: Atmospheres, 109, n/a-n/a, 10.1029/2003jd003957, 2004.

Haywood, J. M., Pelon, J., Formenti, P., Bharmal, N., Brooks, M., Capes, G., Chazette, P., Chou, C., Christopher, S., Coe, H., Cuesta, J., Derimian, Y., Desboeufs, K., Greed, G., Harrison, M., Heese, B., Highwood, E. J., Johnson, B., Mallet, M., Marticorena, B., Marsham, J., Milton, S., Myhre, G., Osborne, S. R., Parker, D. J., Rajot, J. L., Schulz, M., Slingo, A., Tanré, D., and Tulet, P.: Overview of the Dust and Biomass-burning Experiment and African Monsoon Multidisciplinary Analysis Special Observing Period-0, Journal of Geophysical Research, 113, 10.1029/2008jd010077, 2008.

Hong S., D. J., and Shu–Hua Chen S.: A revised approach to ice microphysical processes for the bulk parameterization of clouds and precipitation, Mon. Wea. Rev, 132, 103-120, https://journals.ametsoc.org/view/journals/mwre/132/1/1520-0493_2004_132_0103_aratim_2.0.co_2.xml, 2004.

Hong S., N. Y., Dudhia J.: : A new vertical diffusion package with an explicit treatment of entrainment processes, Mon. Wea. Rev, 134, 2318–2341, https://journals.ametsoc.org/view/journals/mwre/134/9/mwr3199.1.xml,, 2006.

Kerandi, N., Arnault, J., Laux, P., Wagner, S., Kitheka, J., and Kunstmann, H.: Joint atmospheric-terrestrial water balances for East Africa: a WRF-Hydro case study for the upper Tana River basin, Theoretical and Applied Climatology, 131, 1337-1355, 10.1007/s00704-017-2050-8, 2017.

Kerandi, N. M., Laux, P., Arnault, J., and Kunstmann, H.: Performance of the WRF model to simulate the seasonal and interannual variability of hydrometeorological variables in East Africa: a case study for the Tana River basin in Kenya, Theoretical and Applied Climatology, 130, 401-418, 10.1007/s00704-016-1890-y, 2016.

Kinney, P. L., Gichuru, M. G., Volavka-Close, N., Ngo, N., Ndiba, P. K., Law, A., Gachanja, A., Gaita, S. M., Chillrud, S. N., and Sclar, E.: Traffic Impacts on PM(2.5) Air Quality in Nairobi, Kenya, Environ Sci Policy, 14, 369-378, 10.1016/j.envsci.2011.02.005, 2011.

Kume, A., Charles, K., Berehane, Y., Anders, E. and Ali, A.: Magnitude and variation of traffic air pollution as measured by CO in the City of Addis Ababa, Ethiopia, Ethiopian Journal of Health Development, 24, https://doi.org/10.4314/ejhd.v24i3.68379, 2010.

Lacaux, J. P., Brustet, J.M., Delmas, R. et al.: Biomass burning in the tropical savannas of Ivory Coast: An overview of the field experiment Fire of Savannas (FOS/DECAFE 91), J Atmos Chem, 22, 195–216, https://doi.org/10.1007/BF00708189, 1995.

Li, C., Martin, R. V., van Donkelaar, A., Boys, B. L., Hammer, M. S., Xu, J. W., Marais, E. A., Reff, A., Strum, M., Ridley, D. A., Crippa, M., Brauer, M., and Zhang, Q.: Trends in Chemical Composition of Global and Regional Population-Weighted Fine Particulate Matter Estimated for 25 Years, Environ Sci Technol, 51, 11185-11195, 10.1021/acs.est.7b02530, 2017.

Liousse, C., Guillaume, B., Grégoire, J. M., Mallet, M., Galy, C., Pont, V., Akpo, A., Bedou, M., Castéra, P., Dungall, L., Gardrat, E., Granier, C., Konaré, A., Malavelle, F., Mariscal, A., Mieville, A., Rosset, R., Serça, D., Solmon, F., Tummon, F., Assamoi, E., Yoboué, V., and Van Velthoven, P.: Updated African biomass burning emission inventories in the framework of the AMMA-IDAF program, with an evaluation of combustion aerosols, Atmospheric Chemistry and Physics, 10, 9631-9646, 10.5194/acp-10-9631-2010, 2010.

Liousse, C., Assamoi, E., Criqui, P., Granier, C., & Rosset, R.: Explosive growth in African combustion emissions from 2005 to 2030, Environmental Research Letters, 9, https://doi.org/10.1088/1748-9326/9/3/035003, 2014.

Mailler, S., Menut, L., Khvorostyanov, D., Valari, M., Couvidat, F., Siour, G., Turquety, S., Briant, R., Tuccella, P., Bessagnet, B., Colette, A., Létinois, L., Markakis, K., and Meleux, F.: CHIMERE-2017: from urban to hemispheric chemistry-transport modeling, Geoscientific Model Development, 10, 2397-2423, 10.5194/gmd-10-2397-2017, 2017.

Marais, E. A., and Wiedinmyer, C.: Air Quality Impact of Diffuse and Inefficient Combustion Emissions in Africa (DICE-Africa), Environ Sci Technol, 50, 10739-10745, 10.1021/acs.est.6b02602, 2016.

Marais, E. A., Silvern, R. F., Vodonos, A., Dupin, E., Bockarie, A. S., Mickley, L. J., and Schwartz, J.: Air Quality and Health Impact of Future Fossil Fuel Use for Electricity Generation and Transport in Africa, Environ Sci Technol, 53, 13524-13534, 10.1021/acs.est.9b04958, 2019.

Markakis, K., Valari, M., Perrussel, O., Sanchez, O., and Honore, C.: Climate-forced air-quality modeling at the urban scale: sensitivity to model resolution, emissions and meteorology, Atmospheric Chemistry and Physics, 15, 7703-7723, 10.5194/acp-15-7703-2015, 2015.

Mbewu, A., Mbanya, J.C., : Disease and Mortality in Sub-Saharan Africa, in: Cardiovascular disease edited by: Bank, W., 2006.

Nenes, A., Pilinis, C., Pandis, S.: : Isorropia: a new thermodynamic model for inorganic multicomponent atmospheric aerosols., Aquat. Geochem, 4, 123-152, https://doi.org/10.1023/A:1009604003981, 1998.

Ngo, N. S., Gatari, M., Yan, B., Chillrud, S. N., Bouhamam, K., and Kinneym, P. L.: Occupational exposure to roadway emissions and inside informal settlements in sub-Saharan Africa: A pilot study in Nairobi, Kenya, Atmos Environ (1994), 111, 179-184, 10.1016/j.atmosenv.2015.04.008, 2015.

Ogega O.M., W. H. N., Mbugua J: Exploring the Future of Nairobi National Park in a Changing Climate and Urban Growth., in: The Geography of Climate Change Adaptation in Urban Africa., edited by: Macmillan, P., 2019. https://open.africa/dataset/kenya-administrative-boundaries/resource/b5bee56d-b7cb-4f23-8f2b-356ca0044bf3, 2018.

Pai, S. J., Heald, C. L., Pierce, J. R., Farina, S. C., Marais, E. A., Jimenez, J. L., Campuzano-Jost, P., Nault, B. A., Middlebrook, A. M., Coe, H., Shilling, J. E., Bahreini, R., Dingle, J. H., and Vu, K.: An evaluation of global organic aerosol schemes using airborne observations, Atmospheric Chemistry and Physics, 20, 2637-2665, 10.5194/acp-20-2637-2020, 2020.

Parkin, D. M., Sitas, F., Chirenje, M., Stein, L., Abratt, R., and Wabinga, H.: Part I: Cancer in Indigenous Africans—burden, distribution, and trends, The Lancet Oncology, 9, 683-692, 10.1016/s1470-2045(08)70175-x, 2008.

Peña, M. a. R., A.: Environmental Exposures and Cardiovascular Disease, Cardiology clinics, 35, 71-86, https://doi.org/10.1016/j.ccl.2016.09.001, 2017.

Petkova, E. P., Jack, D. W., Volavka-Close, N. H., and Kinney, P. L.: Particulate matter pollution in African cities, Air Quality, Atmosphere and Health, 6, 603-614, https://doi.org/10.1007/s11869-013-0199-6, 2013.

Pohl, B., Crétat, J., and Camberlin, P.: Testing WRF capability in simulating the atmospheric water cycle over Equatorial East Africa, Climate Dynamics, 37, 1357-1379, 10.1007/s00382-011-1024-2, 2011.

Pope, F. D., Gatari, M., Ng'ang'a, D., Poynter, A., and Blake, R.: Airborne particulate matter monitoring in Kenya using calibrated low-cost sensors, Atmospheric Chemistry and Physics, 18, 15403-15418, 10.5194/acp-18-15403-2018, 2018.

Powers, J. G., Klemp, J.B., Skamarock, W.C., Davis, C.A., Dudhia, J., Gill, D.O., Coen, J.L., Gochis, D.J., Ah madov, R., Peckham, S.E., Grell, G.A., Michalakes, J., Trahan, S., Benjamin, S.G., Alexander, C.R., Di mego, G.J., Wang, W., Schwartz, C.S., Romine, G.S., Liu, Z., Snyder, C., Chen, F., Barlage, M.J., Yu, W., Duda, M.G.: : The weather research and forecasting model: overview, system efforts, and future directions, Bull. Am. Meteorol. Soc., 98, 1717–1737, https://doi.org/10.1175/BAMS-D-15-00308.1, 2017.

Pun, B. K., Seigneur, C., and Lohman, K.: Modeling secondary organic aerosol formation via multiphase partitioning with molecular data, Environ. Sci. Technol., 40, 4722–4731, https://doi.org/10.1021/es0522736, 2006.

Real, E., and Sartelet, K.: Modeling of photolysis rates over Europe: impact on chemical gaseous species and aerosols, Atmospheric Chemistry and Physics, 11, 1711-1727, 10.5194/acp-11-1711-2011, 2011.

Schwander, S., Okello, C. D., Freers, J., Chow, J. C., Watson, J. G., Corry, M., and Meng, Q.: Ambient particulate matter air pollution in Mpererwe District, Kampala, Uganda: a pilot study, J Environ Public Health, 2014, 763934, 10.1155/2014/763934, 2014.

Seinfeld, J. H., Pandis, S.N.: Atmospheric chemistry and physics: from air pollution to climate change, edited by: Sons, J. W., 2016.

Singh, A., Avis, W. R., and Pope, F. D.: Visibility as a proxy for air quality in East Africa, Environmental Research Letters, 15, 10.1088/1748-9326/ab8b12, 2020.

Singh, A., Ng'ang'a, D., Gatari, M., Kidane, A. W., Alemu, Z., Derrick, N., Webster, M. J., Bartington, S., Thomas, N., Avis, W. R., and Pope, F.: Air quality assessment in three East African cities using calibrated low-cost sensors with a focus on road-based hotspots, Environmental Research Communications, 10.1088/2515-7620/ac0e0a, 2021.

Skamarock, W., Klemp, J., Dudhia, J., Gill, D., Barker, D., Duda, M., Huang, X., Wang, W., Powers, J., : A description of the advanced research WRF version 3. NCAR, 2008.

Teklay, A., Dile, Y. T., Asfaw, D. H., Bayabil, H. K., and Sisay, K.: Impacts of land surface model and land use data on WRF model simulations of rainfall and temperature over Lake Tana Basin, Ethiopia, Heliyon, 5, e02469, 10.1016/j.heliyon.2019.e02469, 2019.

Telford, P. J., Abraham, N. L., Archibald, A. T., Braesicke, P., Dalvi, M., Morgenstern, O., O'Connor, F. M., Richards, N. A. D., and Pyle, J. A.: Implementation of the Fast-JX Photolysis scheme (v6.4) into the UKCA component of the MetUM chemistry-climate model (v7.3), Geoscientific Model Development, 6, 161-177, 10.5194/gmd-6-161-2013, 2013.

Tewari, M., F. Chen, W. Wang, J. Dudhia, M. A. LeMone, K. Mitchell, M. Ek, G. Gayno, J. Wegiel, and R. H. Cuenca,: Implementation and verification of the unified NOAH land surface model in the WRF model. InProceedings of the 20th Conference on Weather Analysis and Forecasting, 16th Conference on Numerical Weather Prediction, Seattle, 2004.

Thompson A. M., W. J. C., Hudson R. D., Guo H., Herman J. R., and Fujiwara M.: Tropical tropospheric ozone and biomass burning Science, 291, 2128-2132, 10.1126/science.291.5511.2128, 2001.

New Urban Agenda http://habitat3.org/wp-content/uploads/NUA-English.pdf, 2017.

Valari, M., and Menut, L.: Transferring the heterogeneity of surface emissions to variability in pollutant concentrations over urban areas through a chemistry-transport model, Atmospheric Environment, 44, 3229-3238, 10.1016/j.atmosenv.2010.06.001, 2010.

Van Leer, B.: Towards the ultimate conservative difference scheme. V. A second-order sequel to Godunov's method. , Journal of Computational Physics, 32, 101–136, 10.1016/0021-9991(79)90145-1, 1979.

van Loon, M., Vautard, R., Schaap, M., Bergström, R., Bessagnet, B., Brandt, J., Builtjes, P. J. H., Christensen, J. H., Cuvelier, C., Graff, A., Jonson, J. E., Krol, M., Langner, J., Roberts, P., Rouil, L., Stern, R., Tarrasón, L., Thunis, P., Vignati, E., White, L., and Wind, P.: Evaluation of long-term ozone simulations from seven regional air quality models and their ensemble, Atmospheric Environment, 41, 2083-2097, 10.1016/j.atmosenv.2006.10.073, 2007.

Vautard, R., Builtjes, P. H. J., Thunis, P., Cuvelier, C., Bedogni, M., Bessagnet, B., Honoré, C., Moussiopoulos, N., Pirovano, G., and Schaap, M.: Evaluation and intercomparison of Ozone and PM10 simulations by several chemistry transport models over four European cities within the CityDelta project, Atmospheric Environment, 41, 173-188, 10.1016/j.atmosenv.2006.07.039, 2007.

Vliet, V. E. a. K., P.:: Impacts of roadway emissions on urban particulate matter concentrations in sub-Saharan Africa: new evidence from Nairobi, Kenya, Environmental Scientific letters, 2, https://doi:10.1088/1748-9326/2/4/045028, 2007.

Voulgarakis, A., Savage, N. H., Wild, O., Carver, G. D., Clemitshaw, K. C., Pyle, J. A.: Upgrading photolysis in the PHOTOMCAT CTM: model evaluation and assessment of the role of clouds, Geoscientific Model Development, 2, 59-72, https://doi.org/10.5194/gmd-2-59-2009, 2009.

WHO: WHO Air quality guidelines for particulate matter, ozone, nitrogen dioxide and sulfur dioxide, 2005.

WHO: Burden of disease from ambient air pollution for 2012, 2012.

WHO: Ambient Air Pollution: A global assessment of exposure and burden of disease, 2016.

Wild, O., Zhu, X., and Prather, J.:: Fast-J: Accurate simulation of the in- and below cloud photolysis in tropospheric chemical models., J. Atmos. Chem, 37, 245-282, https://doi.org/10.1023/A:1006415919030, 2000.

Wu, W.-S., Purser, R.J., Parrish, D.F., : Three-dimensional variational analysis with spatially inhomogeneous covariances., Mon. Weather Rev., 130, 2905–2916, https://doi.org/10.1175/1520-0493(2002)130<2905:TDVAWS>2.0.CO;2, 2002.

Zyryanov, D., Foret, G., Eremenko, M., Beekmann, M., Cammas, J. P., D'Isidoro, M., Elbern, H., Flemming, J., Friese, E., Kioutsioutkis, I., Maurizi, A., Melas, D., Meleux, F., Menut, L., Moinat, P., Peuch, V. H., Poupkou, A., Razinger, M., Schultz, M., Stein, O., Suttie, A. M., Valdebenito, A., Zerefos, C., Dufour, G., Bergametti, G., and Flaud, J. M.: 3-D evaluation of tropospheric ozone simulations by an ensemble of regional Chemistry Transport Model, Atmospheric Chemistry and Physics, 12, 3219-3240, 10.5194/acp-12-3219-2012, 2012.